ACTIVE NANO-STRUCTURED COMPOSITE COATINGS FOR CORROSION AND WEAR PROTECTION OF STEEL

A Thesis

by

YOO SUNG KIM

Submitted to the Office of Graduate Studies of
Texas A&M University
in partial fulfillment of the requirements for the degree of

MASTER OF SCIENCE

Chair of Committee,	Hong Liang
Committee Members,	Xinghang Zhang
	Partha Mukherjee
Head of Department,	Andreas A. Polycarpou

August 2013

Major Subject: Mechanical Engineering

ABSTRACT

In order to obtain sustainable engineering systems, this research investigates surface and interface properties of metals and active nanostructured coatings. The goal is to develop new approaches in order to improve the corrosion resistance and obtain knowledge in reconstruction of worn and/or corroded surfaces. The research will focus on high carbon steels as the substrate. These materials are used in most of industries and vehicles like aircrafts and automobiles.

For anti-corrosion and self-healing applications, the layer-by-layered (LBL) coatings consisting photo-catalytic materials, the corrosion inhibitor, and the polyelectrolyte will be studied. Potential dynamic tests will be carried out in order to characterize the corrosion potential and current.

For wear study, we will develop a metallic composite that has several functions, such as corrosion and wear protection, refresh or reverse worn or corroded surface. Characterization techniques used include optical microscope, surface interferometer, tribometer and the hardness tester.

The ultimate goal of this research is to understand several types of problems on metal surface, such as corrosion and wear, and explore the possible ways to reduce those by using active nano-structured composite coating on metal surface.

DEDICATION

To my mother, my wife and my daughter for making me concentrative on this research and study. To my advisor for making me confident.

ACKNOWLEDGEMENTS

I would like to recognize the support from my committee members, Dr. Xinghang Zhang, Dr. Partha Mukherjee. Special thanks to Dr. Hong Liang, my advisor, who has guided and supported me to be a good and creative researcher.

I would like to acknowledge the financial support by Korea Air Force for my research project.

I would like to thank all the group members in the Surface Science group for their alternate perspectives in my research. The discussions stimulated new ideas of different research topics, which brought me to learn how to think outside of the box. I would like to specially thank to Xingliang He for his great attention and advice in my research. Support by Kennametal was greatly appreciated.

Finally, I would like to recognize the support from my wife and my daughter who have stood by my dream of progressing professionally. Their love and support makes me stronger and their encouragement keeps me persistent for my dream.

TABLE OF CONTENTS

Page

LIST OF FIGURES

Page

LIST OF TABLES

Page

CHAPTER I

INTRODUCTION

This chapter explains the main concept and approach of this research. Basics about healing for corrosion, wear and cracks on the surface of metal, and how corrosion, wear and cracks occurs on metal substrate. Current issues related to corrosion, wear and cracks on metal are described to better understand the reason why this research is needed.

1.1. Metallic materials

Metals such as steels and aluminum alloy have been used in many industrial applications for their superior stiffness and strength as well as their excellent electrical conductivity [1]. Metals are essential for our life because many plants and transportation equipment are made of the same; examples are airplanes, automobiles, and boats. Like any other materials, metals pose some problems such as fracture due to wear or corrosion induced by environment [2, 3]. These problems are costly and tremendous amount of effort has been made in repair and replacement. Figure 1 shows the comparison of the mechanical properties between various materials [1]. Most metals have higher stiffness, strength and resistance to fracture than other materials such as polymers and composites. These properties are the advantages of metals and would be the reasons why metals are broadly used in many fields.

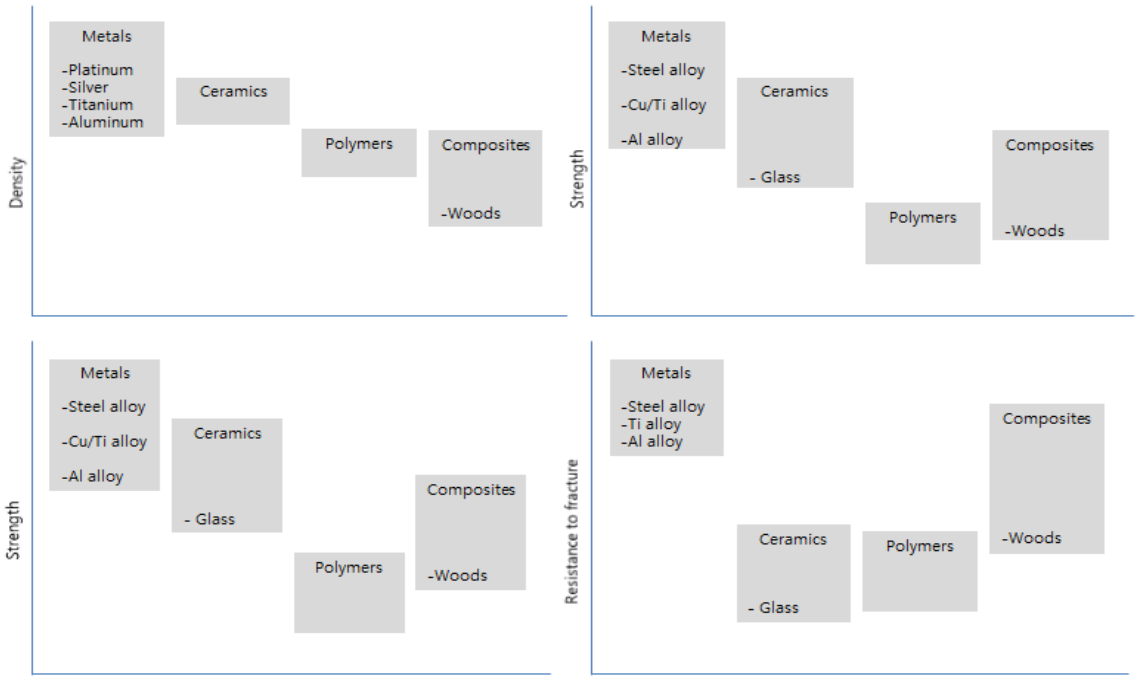

Figure 1. Bar-chart of room-temperature mechanical properties for various metals, ceramics, polymers, and composite materials[1].

Corrosion, wear and cracking are most common causes of failure of metals and they cause problems due to their expense and safety issues of human life [4]. For example, people who are working with aging aircraft are facing to corrosive phenomenon and severe wear and cracks, and that situation brings out many problems such as fracture, malfunction and unexpected troubles [5, 6]. These corrosion, wear and cracking are augmented by surrounding corrosive environment (moisture and salt), excessive and repeated stress on the metals used for aircraft working.

The picture in Figure 2 is a well-known aircraft accident caused by corrosion problem in 1988. Aloha Airlines's Boeing 737 lost most of the upper fuselage in flight, when operating time of this aircraft was only 19 year [5]. At that time, the main problem

was corrosion around the fastener hole to hold the fuselage with the aircraft body and fastener itself [6].

Figure 2. Accident of Aloha airlines aircraft Boeing 737[7]

Beside of this case, there have been many similar cases with this so far, and the cost to repair or overhaul and safety issues have been big problem. Thus, problems related with corrosion have become tremendous.

There are many causes for metallic failure such as corrosion, crack and wear. In order to reduce these metallic failures, engineers can control some factors including a design of product, a choice of materials or a change of environment. If a design of product has defects or errors, this product will fail faster than expected due to applied excessive stress or stress concentrations on a specific spot, which is not designed suitably. If a choice of materials is not proper, the same situation will be happened. For

example, if a metal having low elastic modulus is chosen and excessive stress is applied, the metal will be broken because of its stress-strain relation.

Figure 3 demonstrates the stress-strain curve for high carbon steel and the angle of the stress-strain curve is the elastic modulus of a material in the linear region. Material shows the elastic behavior, meaning it can be recovered to its original shape up to point 1 corresponding to its elastic modulus. The excessive stress that is more than yield stress causes plastic deformation, which cannot be recovered its original shape (from point 1 to 3). The yield strength of a material means the stress which is the material starts plastic deformation. If a stress which is bigger than the ultimate stress is applied, fracture of material will happen. This principle is the basic knowledge to understand the plastic deformation of metals such as wear and crack. Also, proper surface treatments are needed to prevent and minimize these problems because these problems are normally generated from the surface of a material, which can be the reason why surface engineering has been developed.

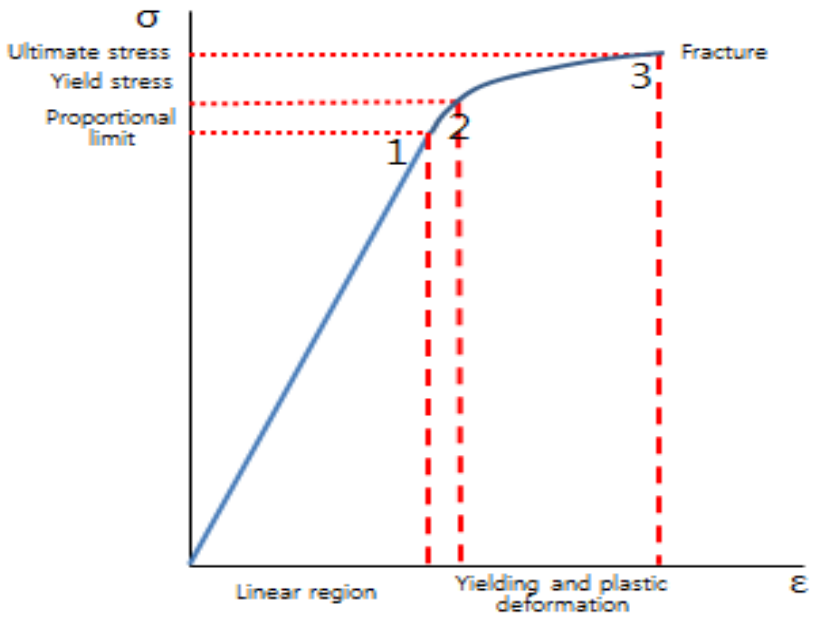

Figure 3. The stress-strain curve for high carbon steel [1]

1.2. Engineering for corrosion and wear resistance

Surface engineering can be explained as mechanical or chemical treatments on the surface of a material for establishing special functions that are known for surface properties such as corrosion resistivity and wear protection. Hence, the surface treatments can extend the service life and improve better performance of materials.

Engine parts of air vehicles are coated with various materials to protect failure of function of parts because the engine parts of air vehicles are exposed to severe conditions such as high temperature, cycled stress causing fatigue or fretting wear and corrosive agents. Several methods of surface treatment have been developed so far in order to obtain proper properties under severe conditions [8].

For example, thermal spray polymer coating for corrosion and PVD magnetron sputtering with MoS_2 to reduce heat energy on transmission parts have been applied for engine parts. A plasma nitriding treatment has been introduced to reduce fatigue problems instead of chromium plating [8].

These surface properties can be modified by mechanical treatment, chemical treatment or constructing of coating and layer on the surface of a materials [9].

1.3. Nature of corrosion

Corrosion is a natural process. All materials want to move to the stable condition that is the lowest energy level thermodynamically, for example water flows from a high level to a low level. Figure 4 shows the cycle for steel product in nature as a simple model [10]. Iron oxide is actually the most stable condition. We can produce steel products by adding energy such as through refining processes. Since a steel product is an unstable condition thermodynamically, it has a tendency to move to the stable level under certain environmental conditions. This is a corrosion reaction on a steel surface. They give up their energy and return to their stable condition thermodynamically and chemically. We usually try to prevent corrosion on surfaces of metals by painting, coating and other surface treatments. If some defects occur on coating, the metal is corroded again. Thus, we need to create a special coating that is self-healable without any effort to discover or repair corrosion on the surface of metals.

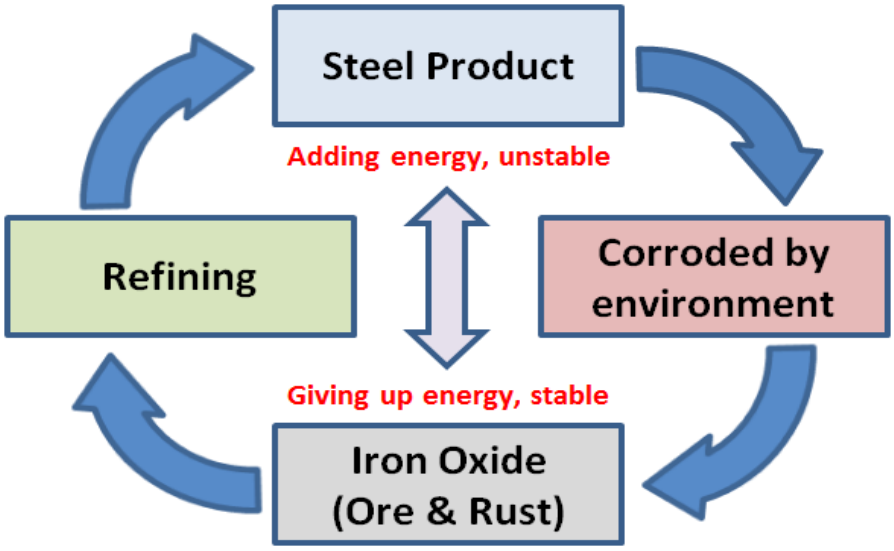

Figure 4. Cycle for steel in nature

Corrosion can be defined as an electro-chemical reaction between materials, usually metals, and surrounding environments. Corrosion on the surface of metals creates a pitting of the surface and makes changes to their properties [10, 11]. Figure 5 is the mechanism of corrosion on a metal substrate by a surrounding environment containing water and oxygen. Metal is decomposed into metal ions and electrons, and then electrons emitted from the metal are combined with water and oxygen in the environment to generate hydroxides. These hydroxides are combined with metal ions to generate metal hydroxides and rust [12]. Thus, the surrounding environmental factors of a metal such as high humidity or salty condition significantly affect its corrosion rate.

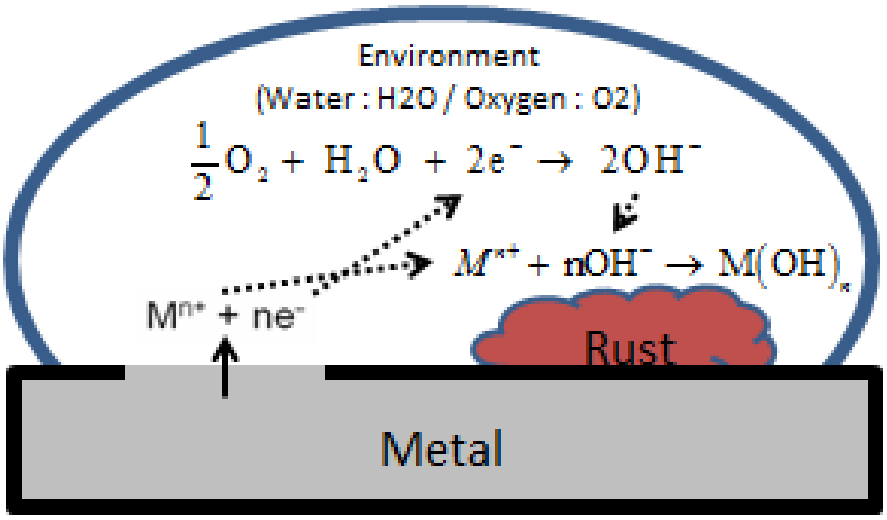

Figure 5. Corrosion mechanism of metal

$$M^o \leftrightarrow M^{n+} + ne^- \quad (1)$$

$$\frac{1}{2}O_2 + H_2O + 2e^- \rightarrow 2OH^- \quad (2)$$

$$M^{n+} + nOH^- \rightarrow M(OH)_n \quad (3)$$

Especially, steel products have been widely used for many fields such as construction of buildings, plants and production of transport equipment due to their high strength, toughness and manufacturability in spite of their vulnerability to corrosion. Several methods for corrosion protection have been developed; the first one is changing metal properties by alloying. The second one is changing the corrosive environment to mild condition. The third one is applying coating on the surface with organic materials or ceramic materials to prevent chemical reaction on the surface of materials by

controlling the electrochemical reaction [9]. Organic surface coating, which is the third one, is common method for corrosion protection such as painting [9].

The organic coatings for anti-corrosion have been developed with various ways and materials such as organic metal polyaniline [13-16]. Some coatings were effective in preventing corrosion, but were less functional with surrounding or were hazardous for the environment sometimes. Organic materials were used to modify surface properties, which might be color, wear protection, insulator or electrochemical reaction [14]. Corrosion means that electrochemical reaction happens between the surfaces of materials, usually metals, and environment, thus organic materials on the surface of metal act as the blocking and the adhesive agent to impede the corrosion reaction. Another important role of the organic materials for anti-corrosion is that it can encapsulate active corrosion inhibitors which are also released under specific conditions [14, 17].

This characteristic of the organic materials will be the important factor for constructing the anti-corrosion and self-healable coating on the surface of the metal in this research, which is the active nano-structured coating with photo-catalytic materials, polyelectrolytes and corrosion inhibitors.

1.4. Principle of wear and cracking

1.4.1. Wear

Wear occurs due to the contact between two or more surfaces and the contact causes the removal or the plastic deformation of a surface owing to the mechanical

performance of the surfaces [18, 19]. Figure 6 shows the mechanism of friction and wear between two different surfaces. Wear may cause a failure of function such as breaking and malfunction.

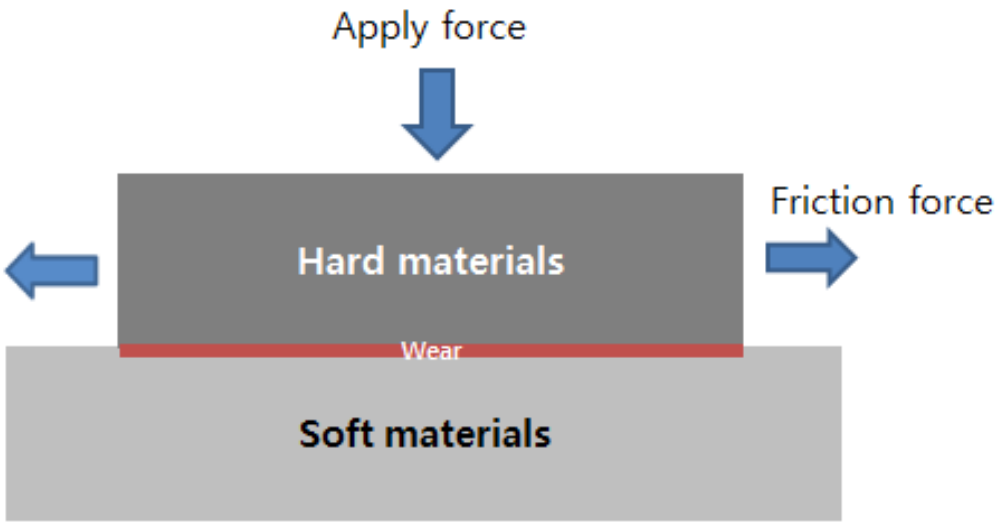

Figure 6. Mechanism of friction and wear

There are mainly four kinds of wear. The first one is adhesive wear that is generated by attachment of wear debris and frictional contact. The second one is abrasive wear that is created by loss of material due to the strong opposite side of the surface with a protrusion [20]. The third one is that the repeated stresses on a surface of materials cause the fatigue wear. This wear happens when materials start to be weakened or detached by the micro-sized cracks, which are caused by the fatigue, cycled stress on the surface of the materials [21]. Finally, similar with the fatigue wear,

fretting wear occurs on the spot where two different surfaces of materials are scrubbed with certain cycle repeatedly [22].

Troubles of wear in industry usually emphasize on abrasive wear that can be divided into two mechanisms [20]. The first one is two-body abrasion which means material is removed by protrusion of the harder material and the second one is three-body abrasion in which separated particles are rolled between the contact of two surfaces [23]. Figure 7 shows the classification of mechanical wear. However, the difference between two-body and three-body abrasion would be vague because the separated particles in three-body abrasion become fixed in one side of the surfaces [20].

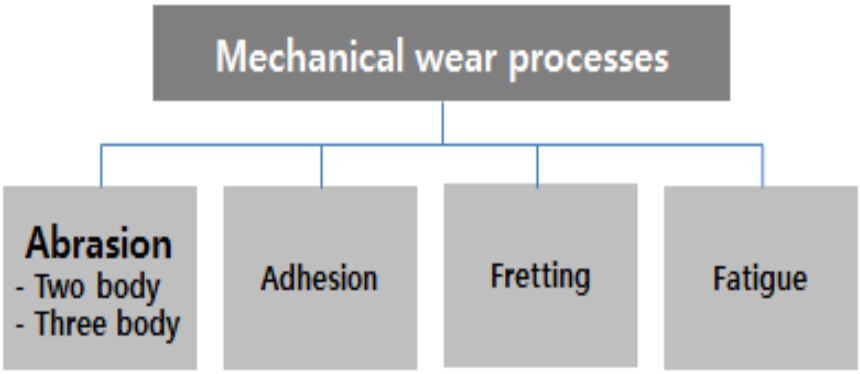

Figure 7. Classification of mechanical wear

There are several methods to improve wear resistivity; the first one is using lubricants to reduce friction energy between the surfaces of materials. The second one is hardening the materials to make the materials harder and strengthen to fracture and

plastic deformation. The third one is preventing corrosion on the surface of the materials, which corrosion causes pitting or erosion on the surface of the materials [9].

For the wear protection, several technic such as mechanical or chemical treatment have been used, for example plating, thermal diffusion, cladding, CVD (chemical vapor deposition) and shot peening. But these technics cause the complex steps and expenses, or severe condition such as high temperature [9].

For example, shot peening is a process to increase service life of materials by cold forming on the surface. Small size of shot impact on the surface of materials, and then compression stressed on the surface is generated which causes impeding of the initiation and growth of the fatigue and fretting wear. But this process needs proper shots with different materials and sizes depending on the applied materials, and special equipment as well as the surface becomes rougher than before treatment due to impact of the shots [8].

In this research, the hardening scheme by using the nano-composite materials under heat treatment will be used to enhance the wear resistivity, which is easy and simple method without any complicate experimental steps and is performed under not severe condition (relatively low temperature).

1.4.2. **Cracking**

Cracking can be defined as a propagated fracture of materials caused by the higher stress than a designed value or repeated stress on materials [24]. Cracking causes

unexpected failures in mechanic, and much expenses and sacrifices of people might have to follow.

Crack initiation occurs on the spots which are the weak points (cause stress concentration) geometrically or the defects like pitting and wear. Crack propagation is generated with the cyclic stress such as the vibration and the loading during operating on the materials in case of the crack caused by fatigue [24, 25]. Figure 8 shows typical crack on the surface of the metal.

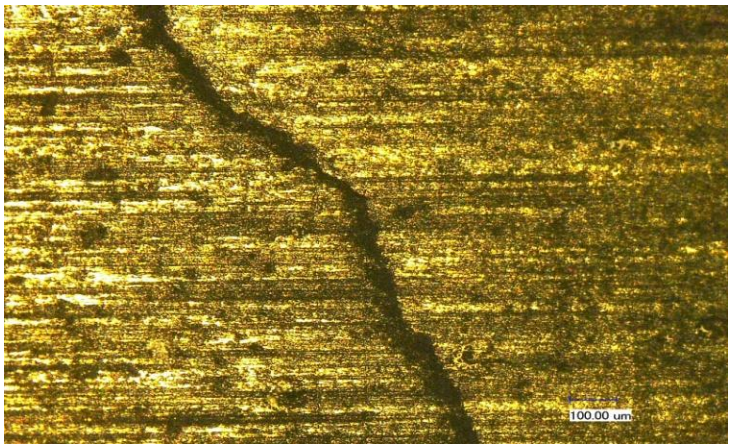

Figure 8. Small crack on the surface of the metal

Figure 9 shows the schematic of crack propagation in materials. A fracture happens due to the propagation of a crack that usually starts from a defect on the surface of materials, even though some cracks start at the middle of a material. A defect on the surface means the surface displacement such as pitting, discontinuity or geometrically weak point. As shown by Figure 9, crack growth direction is developed along with the

defect, and crack growth rate can be different depending on the applied load and direction. Normally, a crack grows faster when a load is applied in perpendicular direction with defect on surface. Hence, a crack growth is influenced by properties of materials, such as Young's modulus, yield strength and stiffness, applied load, shape of materials and defects on the surface.

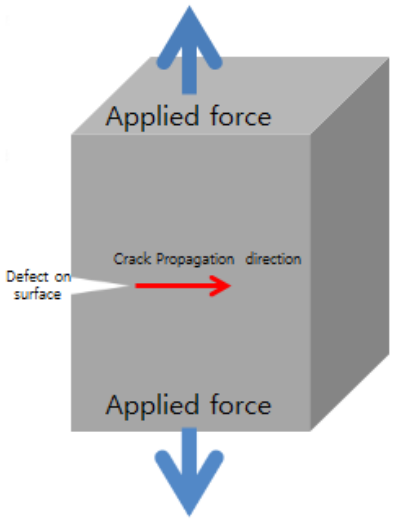

Figure 9. The schematic of crack propagation

One of the most common methods for repairing cracks is welding, but it has several problems. Welding can cause changes in properties of materials, for example the shape or the residual stress for heat of welding or unbalanced heat input. Much labor and cost for repairing are needed. It also requires significant operator skill, thus the quality of welding can vary by technician [26].

1.5. Nanomaterials

Nano-sized materials have several advantages [27]. The first thing is that nanomaterials have higher strength and ductility than conventional materials [28]. The second one is high surface area-volume ratio, which is important factor in chemical reactivity. The nano-sized materials, which have great surface area-volume ratio, can react faster than the conventional materials chemically because the heavy driving power to accelerate thermodynamic process is generated for the nanomaterials [29]. For example, the burning temperature of ultra-fine nano-powder is lower than conventional powder. Thus, some metal nano-powders have been used for rocket propellants and explosives [30]. Figure 10 shows the comparison of surface area-volume ratio according to size. As the material size becomes smaller, the surface area to volume ratio becomes bigger [31].

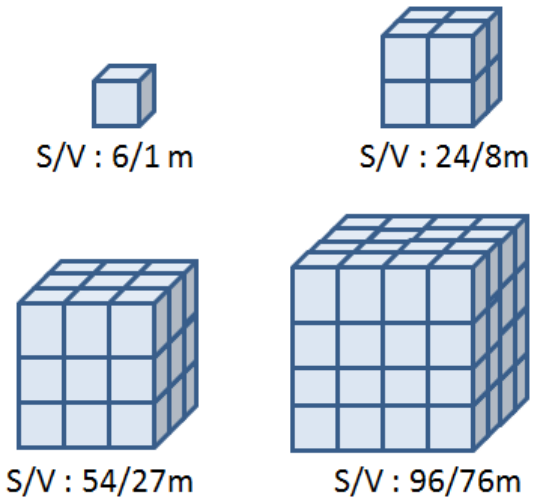

Figure 10. Comparison of surface area-volume ratio according to material size

Figure 11 shows the comparison of surface area-volume ratio according to materials shape. Thus, it can be known that surface area-volume ratio depends on size and shape of materials.

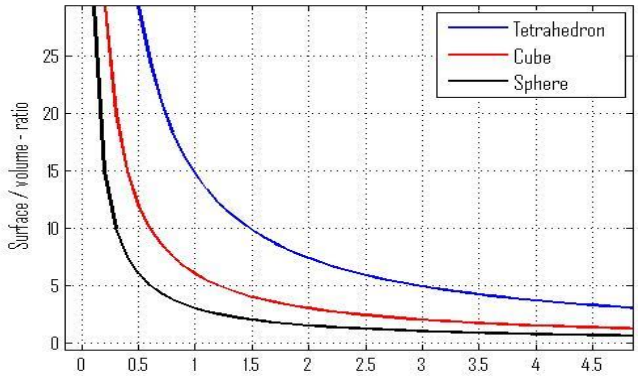

Figure 11. Comparison of surface area-volume ratio according to material shape

1.6. Summary

In this chapter, we discussed reasons why metals have been used widely and their characteristics. Since corrosion, wear and crack are most common problems being occurred in use, we studied mechanisms of those. Corrosion is a natural process and can be defined as electrochemical reaction between metal surface and environment, which may cause pitting or reduction of mechanical properties of metals. Wear happens when two or more surfaces of materials are rubbed against each other with an applied force. A crack is formed and propagated on the spot where geometrically weak point or from a defect on the surface under an excessive applied or repeated stress.

CHAPTER II

MOTIVATION AND OBJECTIVES

As described in CHAPTER I, the problems related with corrosion, wear and cracking on metals are important to any field using metals such as the construction of airplanes, automobiles, ships or buildings for cost and safety reasons. This research aims to develop methods that use critical thinking to overcome those problems. Nano-sized materials are the key for accomplishing the role of healing of metal due to their unique properties of size and surface area to volume ratio. We propose a layer-by-layered coating with the function of photo-catalytic property, the active composite coating for solving the problems.

2.1. Objectives

The goals of this research are to:

- Develop a novel method that can prevent corrosion and can heal the surface through photo-catalytic metal nano-particles as well as inhibitor of corrosion.
- Develop a methodology that can enhance wear resistance on steel substrate by using active metallic nanoparticles.
- Understand mechanisms of property enhancement and surface repair.

These objectives are critical for operating the equipment using metals that are facing problems of corrosion, wear and cracks.

2.2. Dissertation structure

This dissertation presents the corrosion, wear, and cracking phenomenon as well as the main concept and methods for healing these problems in CHAPTER I. The motivations and the objectives are presented in CHAPTER II. Experiments and procedures for preparing the key materials, the techniques and science to repair these problems and evaluation of the healing method are presented in CHAPTER III. Results and discussions of experiments are discussed in CHAPTER IV and V. Conclusions and future work are in CHAPTER VI.

CHAPTER III

EXPERIMENTAL PROCESSURE

This chapter describes experiments to be conducted in this research. It includes materials, corrosion and tribological evaluation, as well as characterization methods. The first part discusses synthesis of layer-by-layered coatings, followed by characterization of materials properties. The second part discussed active composite coating for wear, followed by evaluation of coating. Techniques include AFM (Atomic Force Microscopy), potential dynamic test, electrochemical impedance test, surface morphology tests (optical microscope and surface interferometer). Finally, tribological experiments were conducted in order to assess wear resistivity by hardness, wear rate and friction test.

3.1. The active nano-structured coating for corrosion

3.1.1. Materials

3.1.1.1. Stainless steel

Stainless steel was chosen for the substrate of the active nano-structured coating for corrosion. Stainless steel is prevalent metal in industry due to their comparatively good mechanical properties and low cost. The shortcomings of stainless steels is the localized corrosion and causes the pitting on stainless steel surface by exposure to an environment containing chloride [32].

The type of stainless steel was 316 stainless steel that were composed of Fe (Iron), C (Carbon), Ni (Nickel), Cr (Chromium) and Mo (Molybdenum). This 316 stainless steel has variety of application such as transportation system and architectural fields because it is easy to be manufactured by cutting, rolling of it.

3.1.1.2. **Zinc oxide nano-powder**

Zinc oxide was used as photo-catalytic material which is one of the most popular photocatalytic metal oxides with TiO_2. Its band gap is 3.2 eV. The ultraviolet light, which has 400 – 100 nm wavelength and 3.10 eV – 12.4 eV of energy per photon, needed to react as photocatalytic materials [33-36]. The zinc oxide which used in this experiment was purchased from Sigma Aldrich (<100 nm).

3.1.2. **Sample preparation**

3.1.2.1. **Electrochemical polishing on stainless steel substrate**

Electrochemical polishing (ECP) was performed on the surface of stainless steel. The purpose of electrochemical polishing is to remove an oxidation layer on the surface of substrate and make the surface of sample flat. Mixed solution of 100 ml of perchloric acid and 400 ml of ethanol was prepared, and polishing condition was 25°C and 15 V for 2 minutes. The graphite rod was used for cathode and the stainless steel sample was anode. Figure 12 shows schematic of electrochemical polishing and comparison of surface configuration before and after electrochemical polishing.

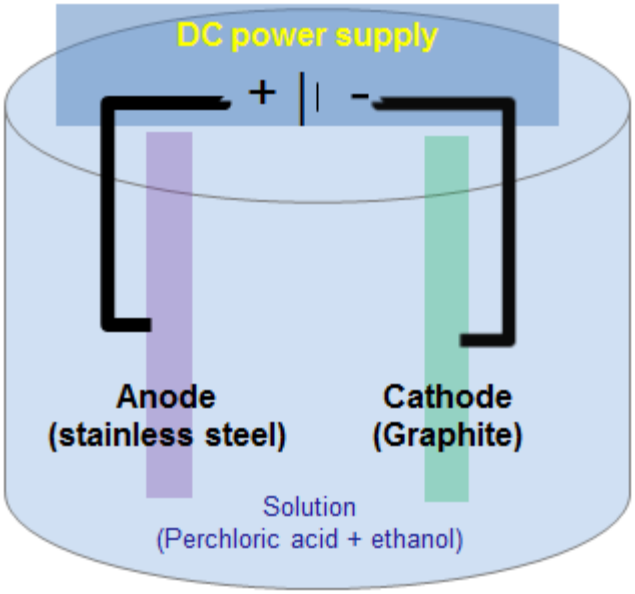

< Schematic of electrochemical polishing >

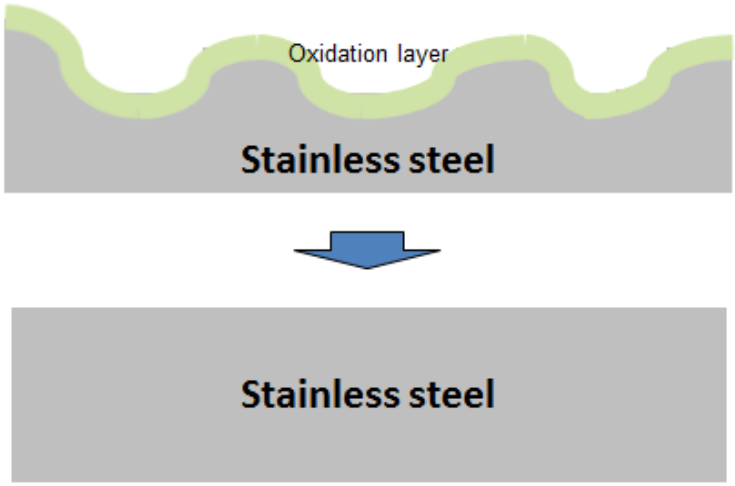

< Comparison between before and after electrochemical polishing >

Figure 12. Schematic of electro-chemical polishing

3.1.2.2. **Coating configuration**

The configuration of the coating was layer-by-layered consisting of photo-catalytic materials, inhibitor for corrosion and polyelectrolytes. The surface protection can be obtained through the formation of a surface film.

To determine coating configuration, we needed to know the surface charge property of coating materials to make attraction force between the coating materials. An active nano-structured composite coating with oppositely charged materials was proposed in order to adhere and adjust the self-healing effects. The surface charge of zinc oxide nano-powders were expected to be negative because negative hydroxyl groups are attached to the surface of nano-oxide typically [37]. Since the corrosion inhibitors, 8-HQ, is positively charged, negatively charged polyelectrolyte, PSS, had to be introduced to encapsulate 8-HQ. PSS and ZnO are negatively charged. PEI, which is positively charged, needed to be introduced to adhere PSS and ZnO [17, 38, 39].

Coating sequence is shown in Figure 13. ZnO was fabricated on the stainless steel substrate, and then PEI was deposited on ZnO. Next, PSS was coated on PEI to capture the corrosion inhibitor (8 HQ). After fabrication of 8 HQ, PSS and PEI were coated on the samples in order.

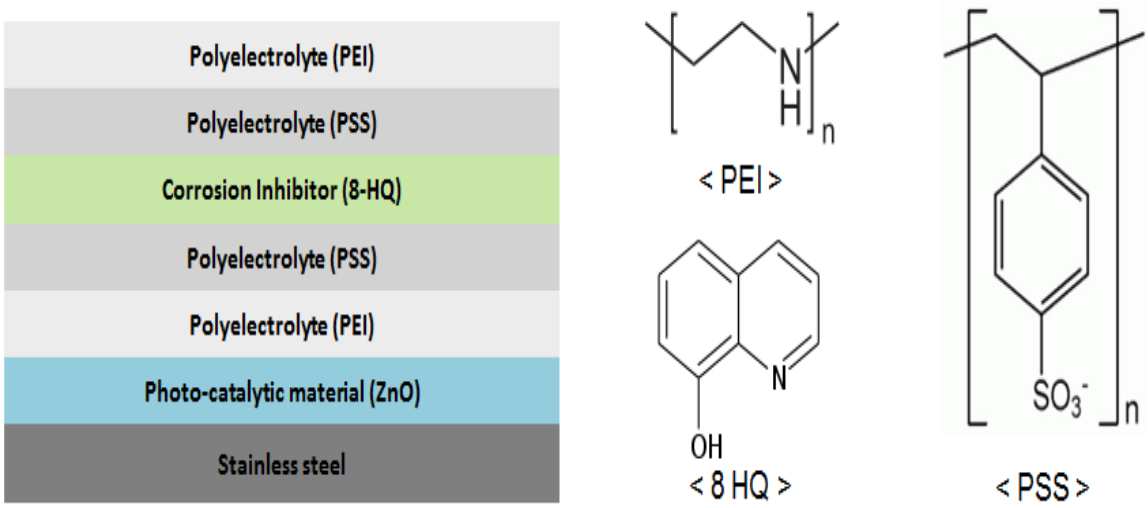

Figure 13. Configuration of layer-by-layered coating

3.1.2.3. **Fabrication of the layer-by-layered coating**

The 0.5g of ZnO nano-powders were dissolved in 50 ml of DI (deionized) water under supersonication for 30 minutes. ZnO nano-powders were coated on stainless steel substrate uniformly by dropping of ZnO solution under 350 rpm for 30 min for 3 times. After ZnO coating, the samples were calcined at 350 ºC for 3 hours in tube furnace with argon gas to prevent contamination. Figures 14 shows the spin coater, and Figures 15 shows the tube furnace that were used.

Figure 14. Spin coater (WS-400-6NPP, Laurell)

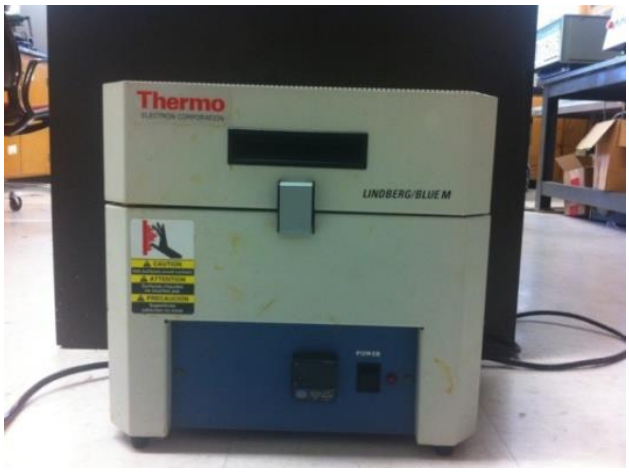

Figure 15. Tube furnace (Thermo Electron Corporation)

The polyelectrolytes, PEI (Polyethyleneimine) and PSS (Poly sodium styrene sulfonate), were purchased from Sigma Aldrich and 0.1 ml of 2mg/mol solution of polyelectrolytes in DI (deionized) water are prepared. PEI and PSS layer were deposited on the sample coated with ZnO under 700 rpm for 30 min, 2 times.

The corrosion inhibitor, 8HQ, was purchased from Sigma Aldrich and 10 wt% solution of 8 HQ in ethanol was prepared. 8 HQ was coated on the sample coated with ZnO, PEI and PSS under 300 rpm for 10 min, 2 times.

3.1.2.4. **Preparation of testing samples**

In order to evaluate the anti-corrosion and self-healing effect of the active nano-structured coating on the stainless steel substrate, four samples were prepared. The first one was the bare stainless steel without any coating materials on it. The second one was the coated stainless steel with the active nano-structured coating. The third one was the damaged stainless steel, which the coating was scratched with sharp blade (damaged). The last one was the healed stainless steel, which the damaged coating was repaired under ultraviolet light. The ultraviolet lighter was set 255 nm wavelengths for 15 minutes. Figure 16 show the ultraviolet lighter that was used.

Figure 16. Ultraviolet lighter (Newport)

Figure 17 shows the surface configuration of each sample (bare, coated, damaged, and healed).

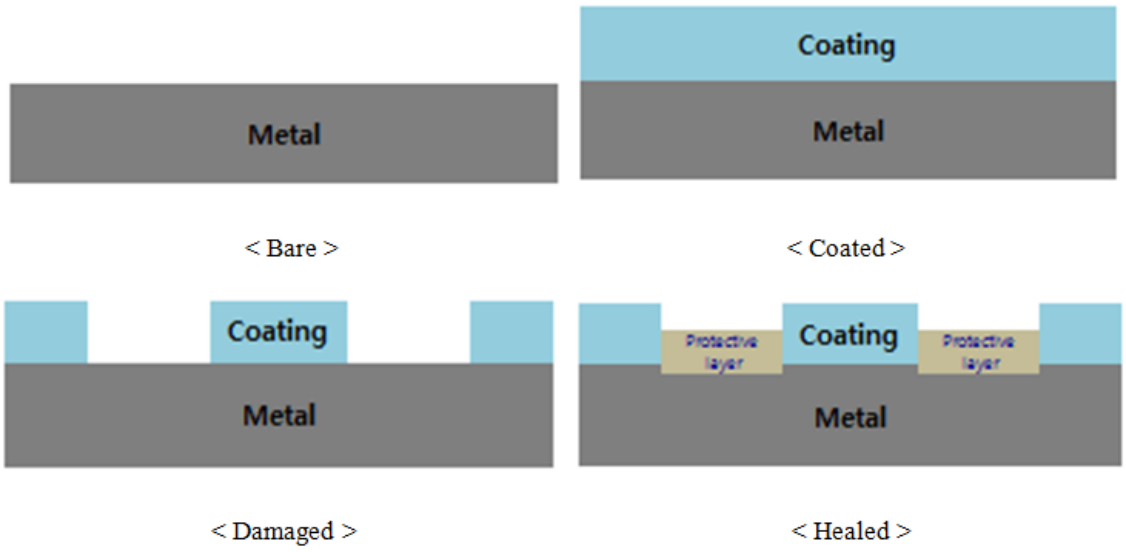

Figure 17. The surface configuration of each sample

3.1.3. Evaluation of the active nano-structured coating for corrosion protection

3.1.3.1. Evaluation of electrochemical polishing by using an AFM

In order to evaluate quality of electrochemical polishing, an AFM (Atomic Force Microscope) was used. The AFM is a powerful to evaluate surface properties of materials such as surface morphology and roughness, adhesion, phase distribution, as well as frictional behavior. It produces high lateral and vertical force resolution by sensing the accurate movement of the AFM probe. Figure 18 shows the schematic of AFM measurement. When the AFM probe scans over a substrate, the photodiode senses

the deflection of the cantilever, which is controlled by the piezoelectric material. Piezoelectric material can change an electric energy to a mechanical energy, which causes precise movement of the AFM probe. Movement of the AFM cantilever is caused by the surface morphology. The laser beam is deflected based on the position of the AFM cantilever. The friction force between the AFM probe and the substrate generates the deflection of the cantilever.

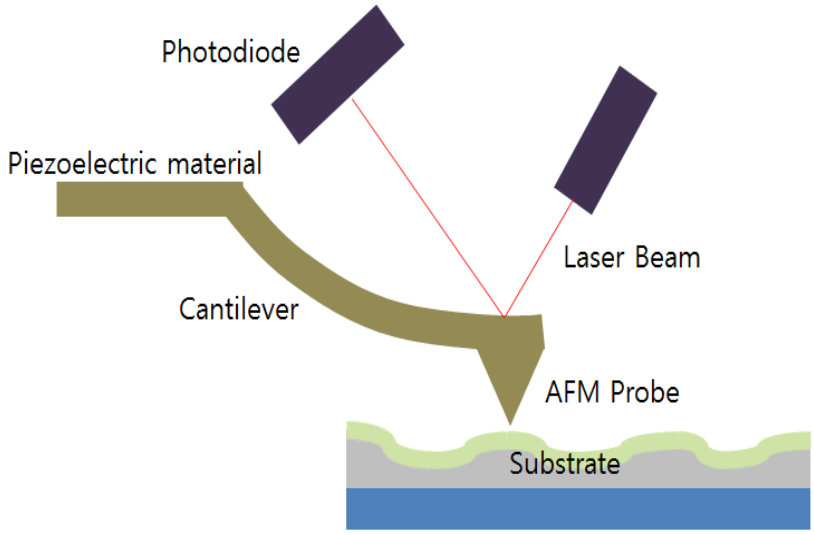

Figure 18. Schematic of AFM measurement

The AFM was used to evaluate the quality of the electro-chemical polishing of the stainless substrate by measuring the surface image and roughness. Figure 19 shows the AFM machine that was used. AFM test was performed with non-contact mode, it measured surface morphology, and AFM tip was made of Silcon Nitrade (Si_3N_4).

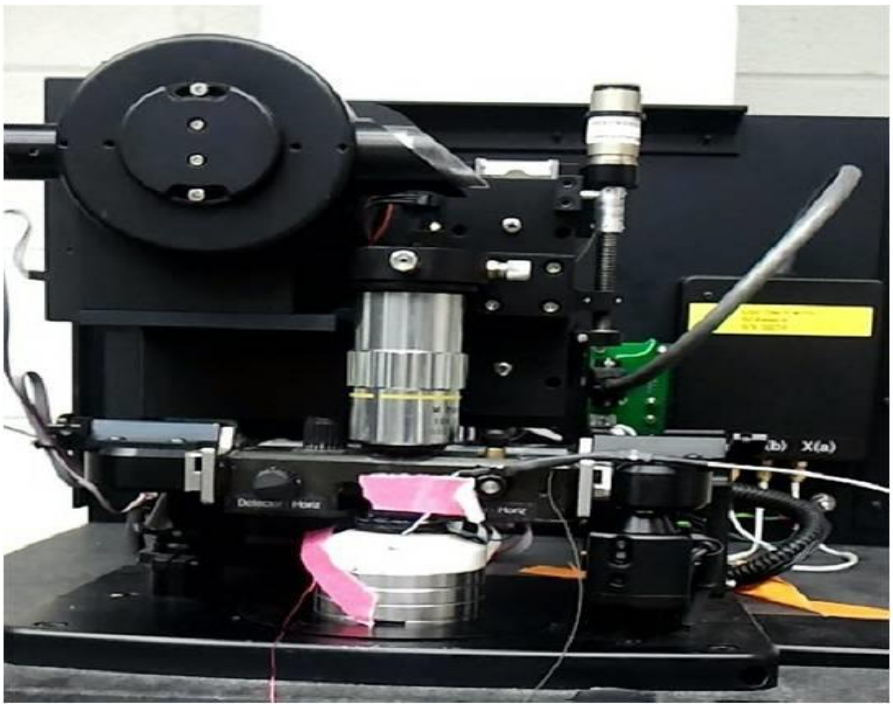

Figure 19. AFM machine (Nano-R AFM, Pacific Nanotechnology Inc.)

3.1.3.2. **Potential dynamic test for evaluation of corrosion resistance**

To evaluate the anti-corrosion ability and self-healing performance of the active nano-structured coating on the stainless steel substrate, potential dynamic polarization tests were performed as corrosion tests. Corrosion begins to happen at the point where the equilibrium state between two electro-chemical reactions, the cathodic and the anodic reaction. The anodic reaction in corrosion can be defined as removing metal ions and electrons from the surface of a sample; this is the oxidation process. The cathodic reaction can be defined as the reduction process.

As applied voltage is increased, the anodic action is increased and the cathodic action is reduced. At the equilibrium point, there is no electrical current, and oxidation and reduction action can take place at the same time. Corrosion potential can be determined at this point, and corrosion occurs above this point. Corrosion current cannot be determined directly, but it can be estimated by finding the extrapolated point between anodic and cathodic curves.

Figure 20 illustrates a polarization curve of a potential dynamic test of a typical metal. The vertical axis shows corrosion potential and the horizontal axis represents corrosion current of a sample. As shown in this figure, the potential dynamic polarization curve can be drawn by adding two reaction curves, the anodic and cathodic curves.

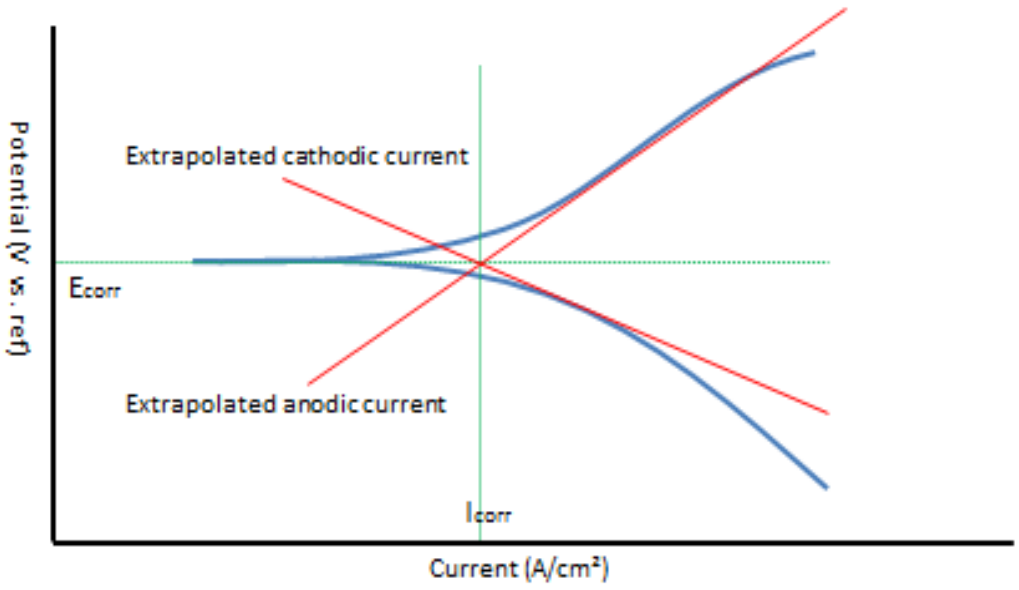

Figure 20. Interpretation of potential dynamic polarization curve

According to this theory, as the potential dynamic polarization curve moves left and up, corrosion resistance of the sample becomes higher. This means that the corrosion of the sample occurs at high potential and corrosion current is also low.

To perform the potential dynamic test, the applied voltage range was -1.5V to 0V with a rate of 1 mV/s, and a corrosive solution of 5 wt% sodium chloride (NaCl) in DI (deionized) water was prepared to mimic sea water. The exposed area of the sample was 0.20 cm^2 and the density of the sample was 8.03 g/cm^3. A Gamry instrument (Reference 600) was used for the test. Figure 21 shows the schematic of potential dynamic test.

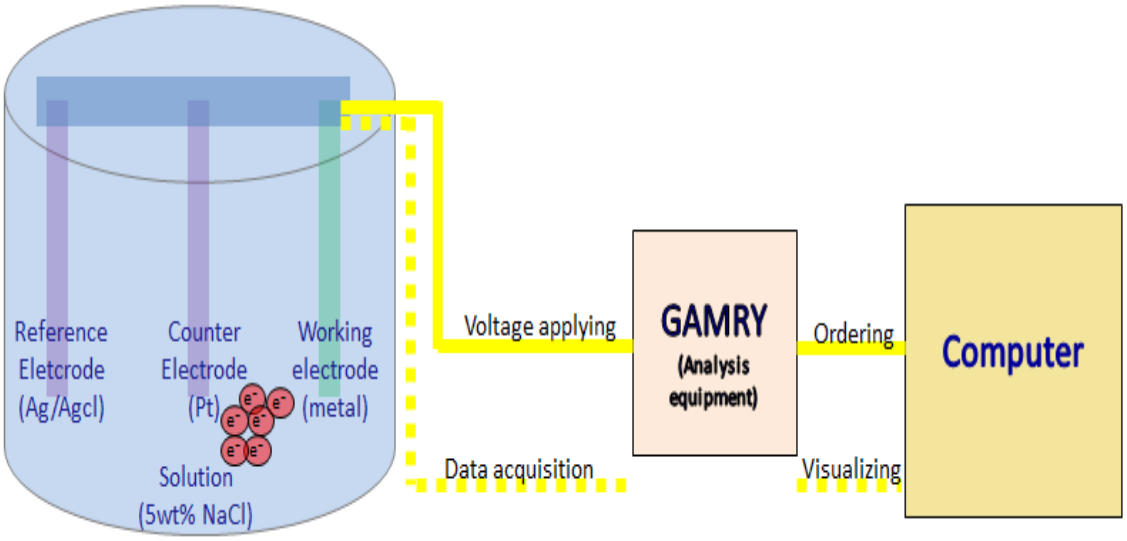

Figure 21. Schematic of potential dynamic test

3.1.3.3. **Electrochemical impedance spectroscopy analysis for evaluation of interfacial interactions for corrosion protection**

EIS (Electrochemical Impedance Spectroscopy) analysis has been performed for evaluation of the interfacial interactions that are the interactions between the surface of metal and the surrounding environment by measuring the impedance corresponding to AC current. This is a useful technique for measuring interface/surface evolution and corrosion reaction of the surfaces [40, 41].

Impedance can be explained as a series of equal electric components, e.g., resistor, capacitor, and inductor, during electrochemical reaction on the material surfaces. The Exact component is highly dependent on the configuration of the surface and interface. It can be identified by calculating the magnitude of impedance and the shape of the graph (nyquist plot, bode plot) [42].

When the AC voltage is applied to the surface of materials with a certain range of frequency, the phase change due to different surface and interface components is measured at the same time. Figure 22 shows the phase change of AC voltage applied.

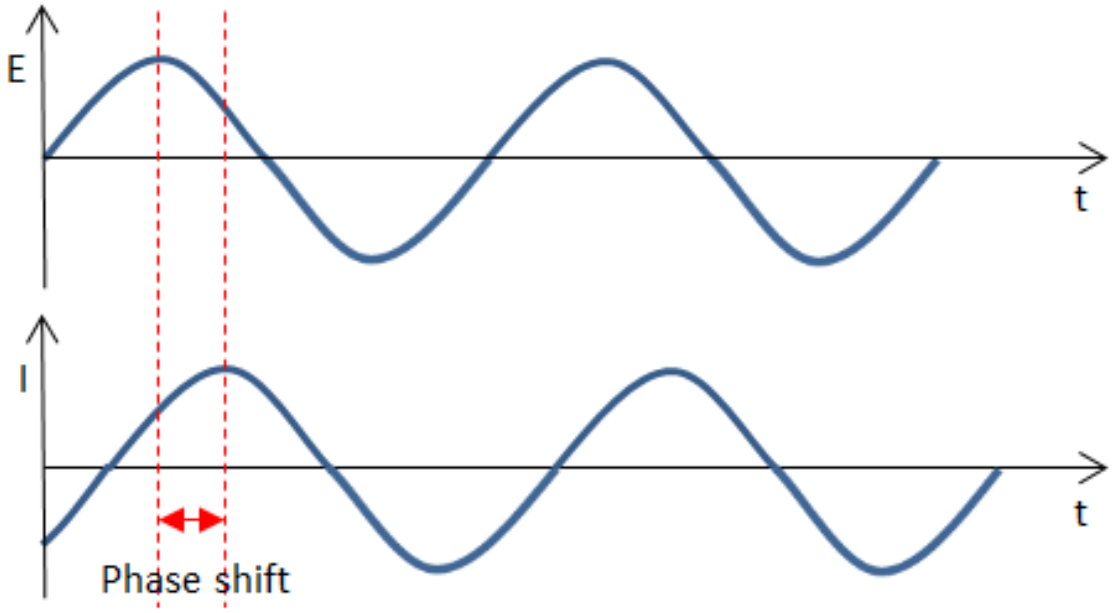

Figure 22. Sinusoidal current response corresponding to applying potential[43]

Impedance (Z) can be explained in following equation, and it contains the real value showing the resistance of the circuit and the imaginary value showing the capacitance of the circuit corresponding to applying frequency.

$$Z(j\omega) = R + jX = R + \frac{1}{j\omega C} = R - j\frac{1}{\omega C} \quad (4)$$

The applying potential and responding current can be express as following equations (when $\omega = 2\pi f$).

$$E_t = E_0 \sin(\omega t) \quad (5)$$

$$I_t = I_0 \sin(\omega t + \theta) \quad (6)$$

By Euler's equation, impedance (Z) can be expressed as the following equation. This equation can be compared with equation (4) to identify the resistance (real value) and the capacitance (imaginary value).

$$Z(\omega) = \frac{E}{I} = Z_0 \exp(j\theta) = Z_0(\cos\theta + j\sin\theta) \tag{7}$$

By equation (9), Nyquist plot can be generated showing impedance (Z) between the electrode and electrolyte in Figure 23 where $R = Z_0 \cos\theta$, and $X = Z_0 \sin\theta$. In nyquist plot, the radius of semicircle indicates the magnitude of impedance.

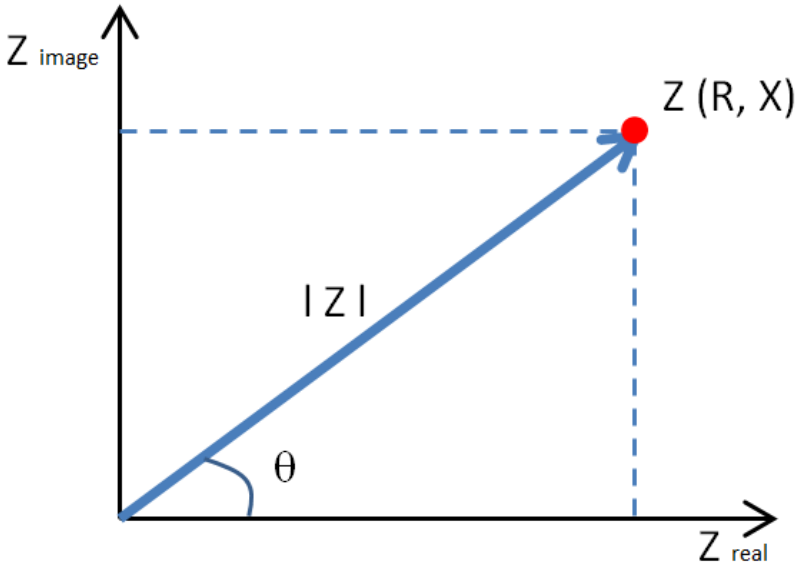

Figure 23. Nyquist plot with impedance vector [43]

In the electrochemical circuit model, there are three special elements: resistor, capacitor and Warburg impedance.

The first is resistor R (Ω) when the phase changes (θ) is zero, it means that the current is in the applying voltage. The physical meaning of this polarization resistance is inversely related to the corrosion rate. Polarizing happens when frequency of applying voltage is becoming low to the electrodes (approaching DC), and then the current flow is caused by the polarization of the electrode that causes the electrochemical reaction at the surface of electrode. For the corrosion reaction, as resistance become higher, the corrosion rate becomes lower by something protective to corrosion.

The second is capacitor when the phase changes (θ) is -90˚. Capacitor is generated when the some dielectric materials impede the current flow between the electrode and environment (electrolyte), for example, double layer on a surface. The double layer generated by charges on the surface of electrode acts as a kind of insulator and forms a capacitor. The ability of a capacitor can be varied with the distance between the electrode and environment (electrolyte), and the ability of the dielectric double layer. As the distance between the electrodes is low and electrical permittivity is high, the value of the capacitor is low.

The third is Warburg impedance that represents the diffusion process between the electrode and environment (electrolyte). The diffusion process happens due to the difference of ionic concentration between the electrode and environment (electrolyte). Normally, the ionic concentration of the electrolyte is much higher than the electrode. Warburg impedance is affected by the frequency of applying voltage. As the frequency of the applying voltage become low, the diffusion of ions can go farther, which is caused by increasing the Warburg impedance.

By measuring of impedance between the electrode and electrolyte, the corrosion resistivity and the surface configuration of materials can be evaluated.

Applying voltage was AC 100 mV that is sinusoidal waveform with a range of frequencies from 0.1 Hz~1 MHz for each test sample.

3.1.4. **Steps to fabricate the active nano-structured coating for corrosion**

Figure 24 explains the experiment steps of active nano-structured coating for corrosion and self-healable coating on the surface of stainless steel.

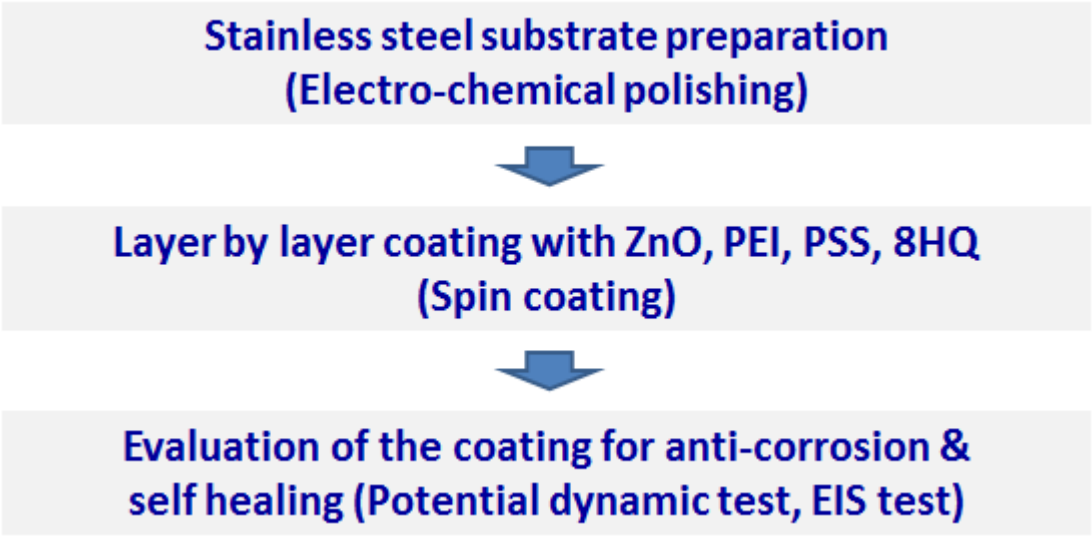

Figure 24. Experiment steps of active nano-structured coating for corrosion

The first step was electro-chemical polishing of the stainless steel substrate. Then, layer-by-layer coating was performed with ZnO, PEI, PSS, 8HQ, PSS and PEI in

order. Finally, potential dynamic test and EIS test were performed to evaluate the corrosion resistance and self-healing effect.

3.2. The active composite coating for wear protection

3.2.1. Materials

3.2.1.1. High carbon steel

The high carbon substrate samples with cracks were used for this study. Image is shown in Figure 25.

Figure 25. The carbon steel sample for active composite coating for wear protection

3.2.1.2. The active composite material

The aluminum nanopowder (from Sigma Aldrich) and the sodium nitrate ($NaNO_3$, from Sigma Aldrich) were used as ignition and releasing agents in active

composite materials. Aluminum nano-powder and sodium nitrate have been added in propellants of solid rocket to enhance the combustion performance due to their own property such as high aspect ratio and an excellent chemical reactivity [44, 45].

The powders of graphite, iron and tungsten (all from Sigma Aldrich) were used as the surface modifiers to increase hardness and wear protection of the carbon steel substrates. Graphite consists of layered structures with carbon atoms which are honeycomb lattice. Carbon acted as a hardening agent of steel. High carbon steel, which has high carbon content, is expected to be harder and stronger than low carbon steel [46]. Iron powder was used to adhere the composite coating materials and the surface of carbon steel substrates. Tungsten was consumed for the production of hard materials and heavy metal alloys due to their high density. Their extremely high hardness makes more resistant for wear [47].

3.2.1.3. **Preparation of the active composite materials**

For the heat ignition and releasing agents, 20 wt% of aluminum nanopowder and 20 wt% of sodium nitrate were used. For the surface modifiers, 20 wt% of graphite powder, 20 wt% of iron powder and 20 wt% of tungsten powder were used. Composite materials were mixed uniformly together in mixer for 8 hours. Figure 26 shows the mixer that was used.

Figure 26. Mixer (Inversion Machines Itd.)

3.2.1.4. **Heat treatment**

The high carbon steel substrate was covered with the mixed composite material. The heat-treatment was performed in furnace for 6 hours at 400ºC to make new hard surface on carbon steel substrate. Figure 27 shows the furnace that was used.

Figure 27. Furnace (F-A1630, Thermolyne Corporation)

3.2.2. **Evaluation of wear resistance**

To examine the surface profile of the high carbon steel, a surface interferometer was used to identify the surface profile before and after the active composite coating. Surface interferometer can measure the surface roughness and makes it easy to visualize with colorful range to examine surface irregularities. Figure 28 shows the 3D optical surface interferometer (ZYGO NEW VIEW 600). A 10x objective was used for measuring of samples, and a vibration isolator was needed to eliminate vibrations from noise that would affect the measurement. After measuring, images (2D, 3D) were created with the surface profiles.

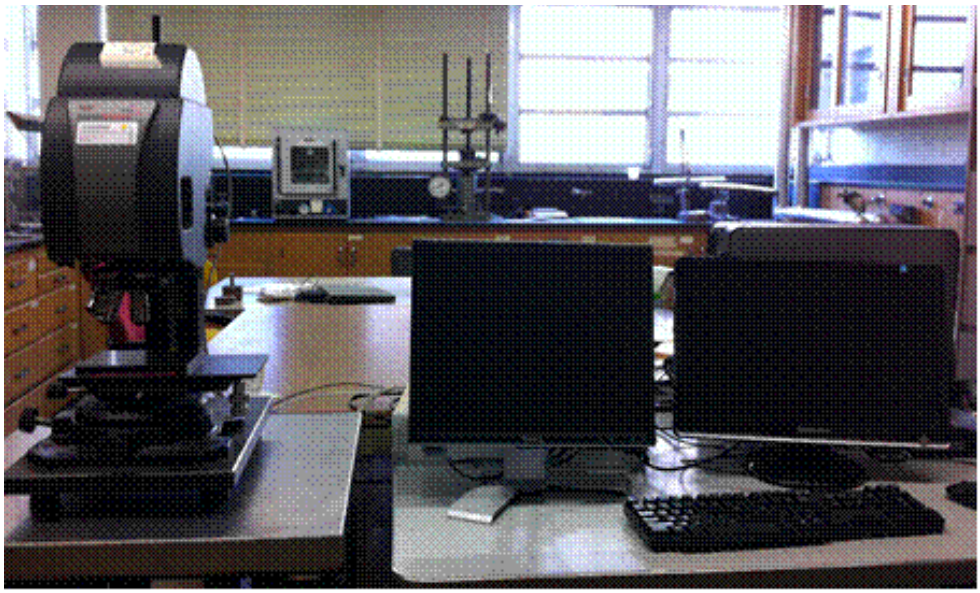

Figure 28. Surface interferometer (ZYGO NEW VIEW 600)

3.2.2.1. **Tribometer**

Tribometers were used to measure tribological features such as friction coefficient and wear resistance for the coated sample and the non-coated sample. In order to measure the friction coefficient of the samples, a pin-on-disk tribometer was used with a reciprocating linear test mode. The selected amplitude was 2 mm, the scanning speed was 12 cm/s, the distance was 100 m, and the applied load was delivered with 4 N using a D52100 bearing ball of 6 mm diameter. In order to make the wear track, 8 lb of weight using a 6 mm D52100 bearing ball for 2 hours was applied. After the tribo-tests, the wear tracks of the samples were examined by the surface interferometer (ZYGO NEW VIEW 600) and the optical microscope (KEYENCE VHX-600K) in order to calculate the worn volume and the wear rate of the samples. Figure 29 shows the tribometer that was used.

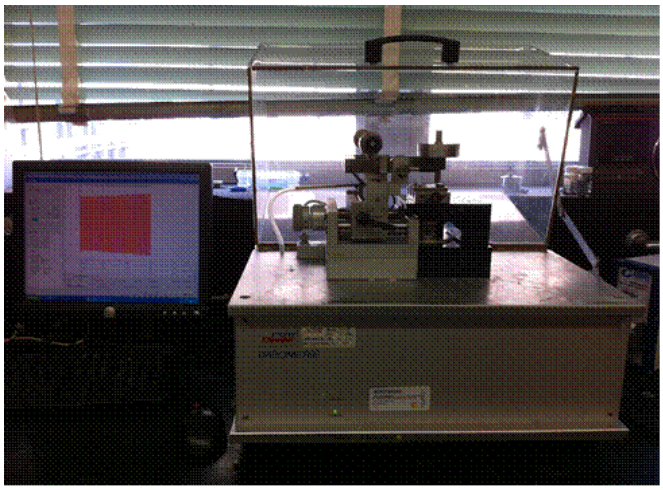

Figure 29. Tribometer for measuring friction coefficient (CSM Instrument)

3.2.2.2. **Hardness test**

Rockwell hardness test is widely used to measure a hardness of materials and the Rockwell scale is determined by measuring the gap of indented depth between a major load and a minor load on a material. The gap of indented depth can be affected by the elastic property of a material [48]. Figure 30 and 31 shows the schematic of Rockwell hardness test and the Rockwell hardness tester that was used. There are several Rockwell scales with dimensionless number; here we use the HRC scale that is used mainly as hard steels.

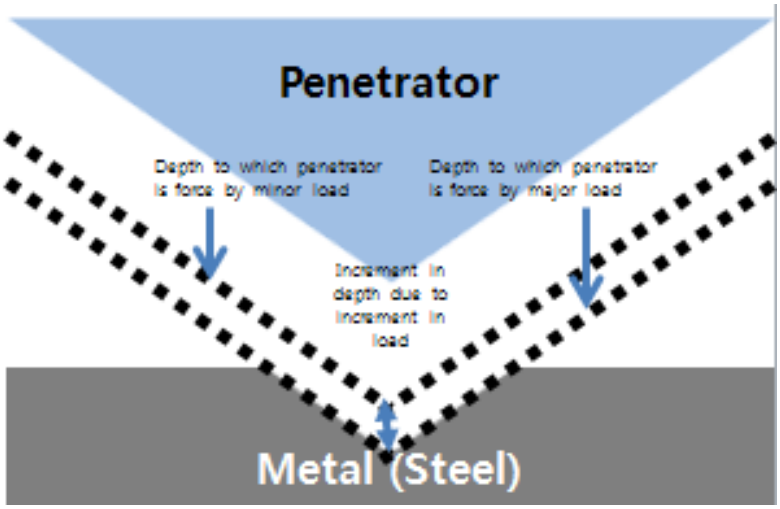

Figure 30. Schematic of Rockwell hardness test [49]

Figure 31. Rockwell hardness test (INSTRON instrument)

3.2.3. **The experiment steps of the active composite coatings for wear protection**

Figure 32 explains the experiment steps for wear resistant coating on the surface of high carbon steel substrate.

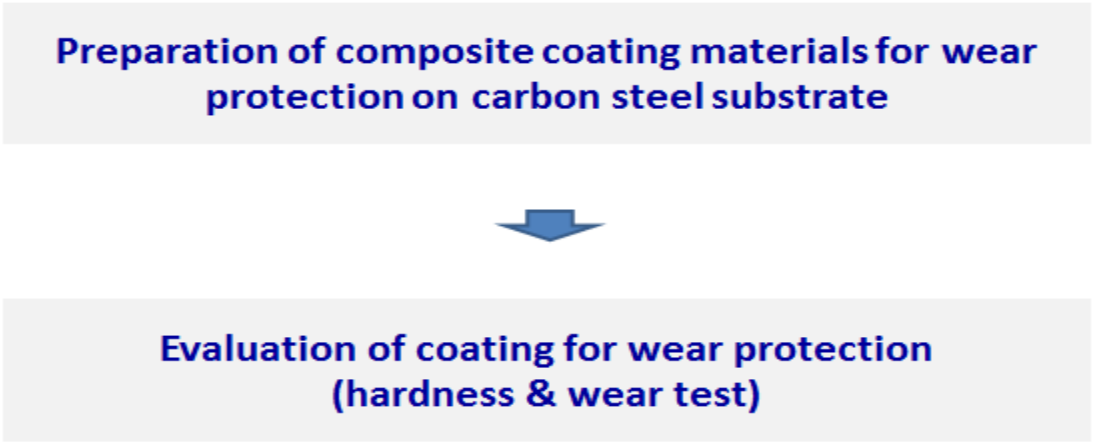

Figure 32. Experiment steps of active the composite coating for wear

The first step was preparation of composite coating materials for wear protection on carbon steel substrate. The second step is evaluation of coating for wear protection by hardness and wear test.

3.3. Summary

This chapter describes the experiment steps for the active nano structured coating for corrosion and self-healing by using ZnO photocatalytic materials, PEI/PSS polyelectrolytes and 8HQ corrosion inhibitor. In order to evaluate the corrosion resistance, potential dynamic test and EIS test were introduced. For wear protection coating on the carbon steel, the active composite coating materials were used. These composite materials were composed of aluminum nano-power, sodium nitrate, graphite, iron and tungsten which are mixed uniformly.

CHAPTER IV

ACTIVE NANO-STURCTURED COATING FOR CORROSION

This chapter discusses the active nano-structured composite coating for corrosion and self-healable coating. To investigate corrosion resistance of the sample, the potential dynamic test was performed under a corrosive condition (salt water).

4.1. AFM result of electrochemical polishing of the stainless steel substrate

By atomic force microscopy tests, the surface morphology of two different samples can be evaluated by comparing 3 D and 2 D images of the surfaces.

As shown in Figure 33, the surface of the electrochemical polished sample became flat. It was hard to find any protrusion or irregularity in the surface of the electrochemical polished sample when comparing it to the surface of the non-polished sample. The surface roughness (Sq) of the non-polished sample was 121.2824 nm, while the surface roughness (Sq) of the polished sample was 31.6376 nm. It is obvious that the electrochemical polishing was accomplished successfully. Surface roughness of stainless steel can effect corrosion resistance. As a surface roughness of stainless steel become lower, corrosion resistance become higher. The rougher surfaces are at risk to generate localized corrosion like propagation of pitting, because a metastable pitting on the stainless steel surface can be led and developed by the surface nucleation [50].

Also, the oxidation layer on the stainless steel surface was expected to be removed during the electrochemical polishing. Oxidation layer on the stainless steel surface may affect the corrosion reaction and the evaluation of the anti-corrosion effect for the active nano-structured coating that was prepared in this research. This is why the electro-chemical polishing was performed.

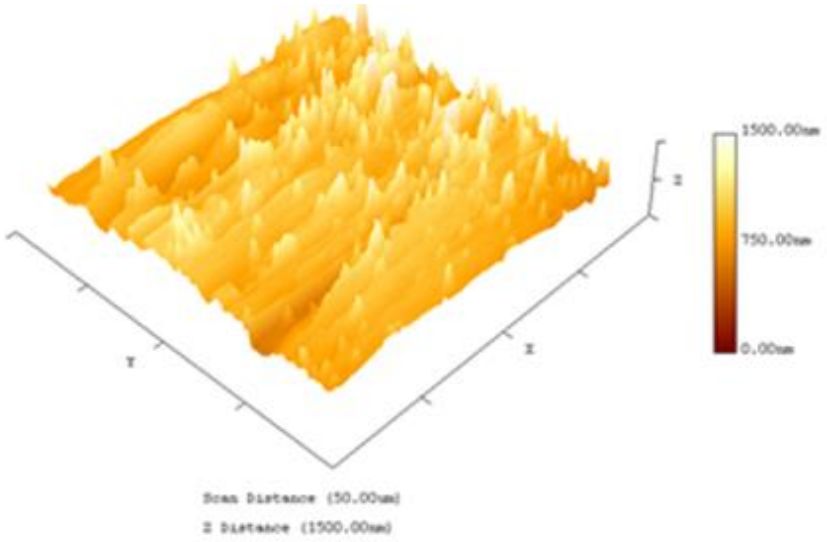

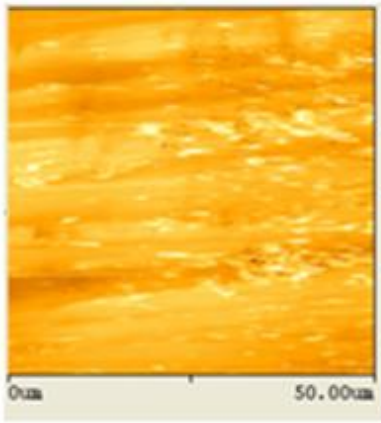

	Whole Area
Total Area St.	2519.5051 um²
Roughness Avg. Sa:	89.6556 nm
Root mean square Sq:	121.2824 nm
Ten Points Height Sz:	1381.9857 nm
Range Sr:	1712.5345 nm

< Before electro-chemical polishing >

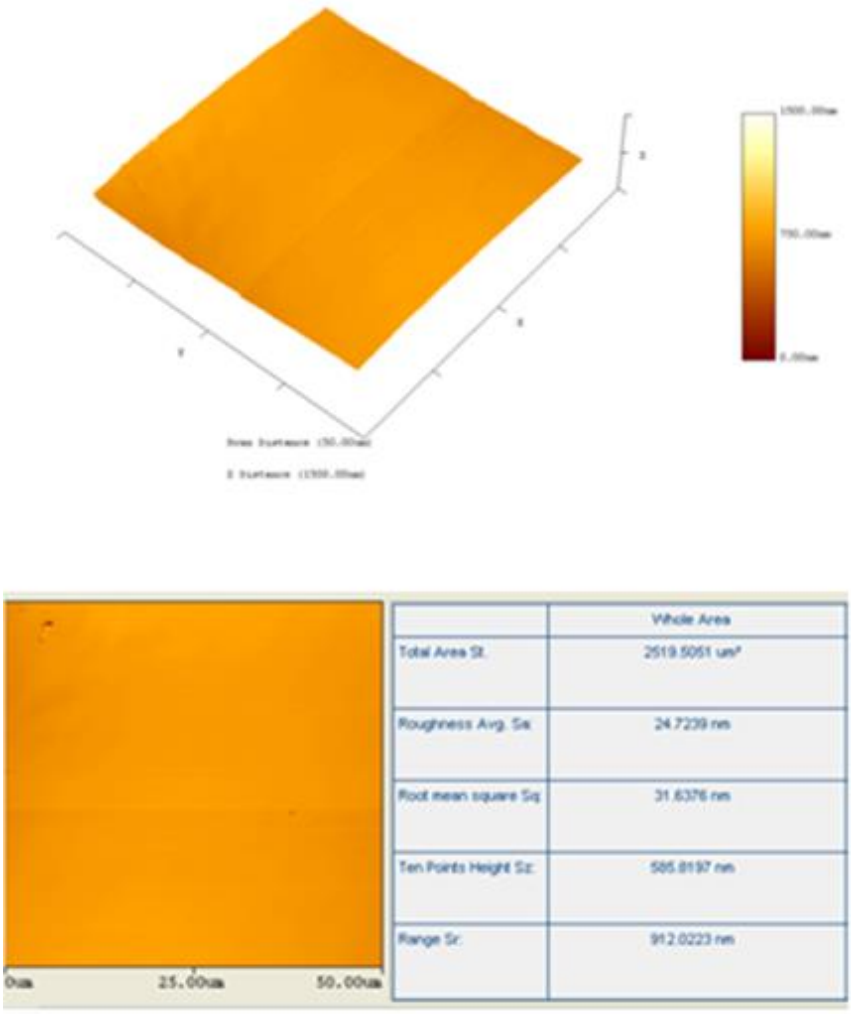

< After electro-chemical polishing >

Figure 33. Comparison of the surface morphology between before and after coating

4.2. Result of potential dynamic test for the samples

A potential dynamic test is performed to determine the corrosion potential and corrosion current under certain environments. These parameters are normally obtained from a potential dynamic curve. As described before, corrosion processes come with

electron and metal ion transfers between a metal surface and a corrosive environment [51]. If the metal shows a higher potential value and a lower current value than other metals, we can assume that the metal has high resistance to corrosion. Normally, high corrosion potential state means stable condition, and low corrosion potential state means active condition.

For the potential dynamic test, stainless steel is used as the substrate and four samples (bare, coated, damaged, and healed) are measured to evaluate the corrosion potential of the anti-corrosion and the self-healing ability of corrosion resistance under 5wt% NaCl water, which is corrosive like sea water.

4.2.1. **Comparison of potential dynamic test between before and after coating**

As shown in Figure 34, potential dynamic curves of the two samples shows their corrosion potential and current. In the case of the bare sample, the corrosion potential and current was determined to be around -0.9 V (vs Vref) and $10^{-4.5}$ A/cm^2. After the coating for anti-corrosion on the stainless steel, the corrosion potential and current was determined to be around -3.7 V (vs Vref) and $10^{-4.25}$ A/cm^2.

The corrosion potential of the coated sample was -0.53 V higher than the bare sample, and the corrosion current of the coated sample was less than the bare one. Therein, it can be concluded that the active nano-structured coating, which was composed of Zinc oxide nano-particles, the corrosion inhibitor and the polyelectrolytes, prevented the corrosion reaction on the stainless steel surface. Zinc oxide nano-powders and the corrosion inhibitors fabricated on the stainless steel surface prevented and

resisted the corrosion reaction, because these materials acted as insulators which prevented an electro-chemical reaction between the electrolyte (corrosive solution) and the stainless steel.

As described in the introduction, a corrosion reaction can be defined as an electro-chemical reaction on a metal surface, which is an anodic passivation reaction. When an anodic passivation reaction dominates the electro-chemical reaction on the metal surface, it can be said that corrosion starts to happen. Corrosion potential value can be determined at this point in which corrosion begins. Thus, it can be said that corrosion on the surface of a metal having a lower corrosion potential happens easier than a high corrosion potential metal.

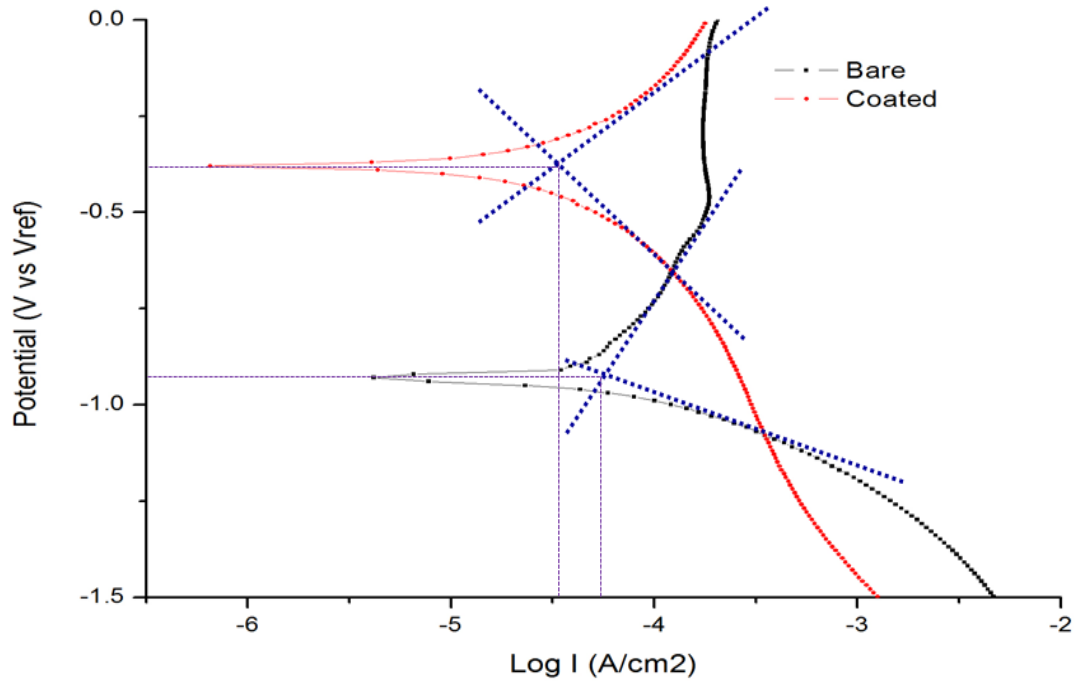

Figure 34. Comparison of the corrosion potential and current between samples (bare, coated)

4.2.2. **Comparison of potential dynamic test between damaged and healed coating**

Figure 35 shows the potential dynamic curves of the two samples, damaged and healed. The damaged sample means that the active nano-structured coating on the stainless steel was scratched by the sharp blade, and the healed sample means that the damaged sample was re-constructed by ultraviolet light (255 nm wavelength, 15 minutes). The ultraviolet light from the light source causes the photo-reaction of Zinc oxide nano-powders which are deposited on the stainless steel substrate uniformly.

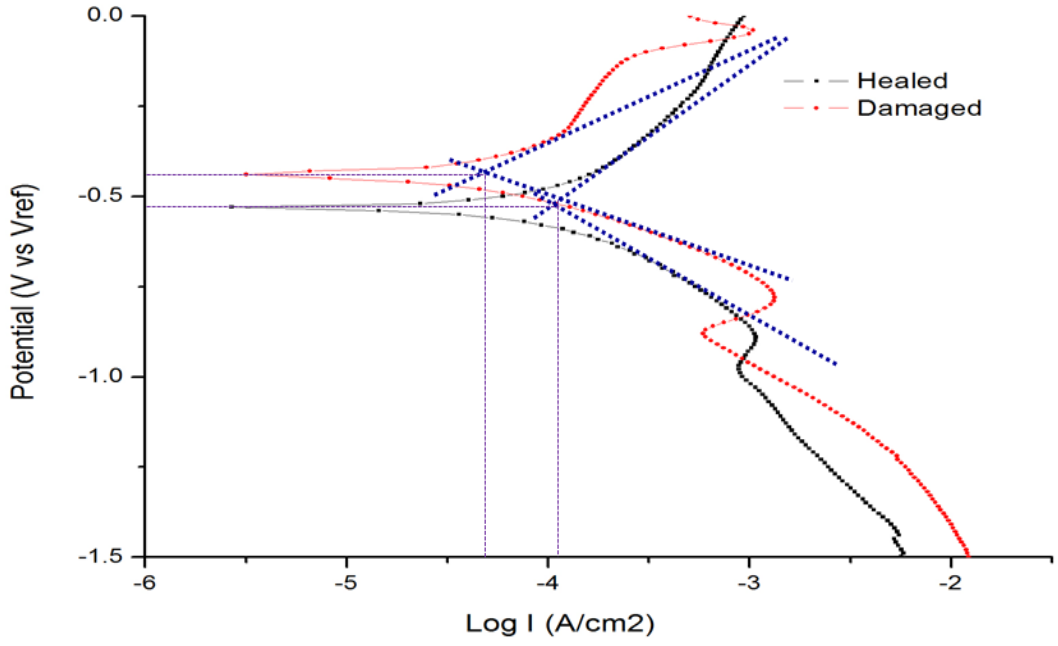

Figure 35. Comparison of the corrosion potential and current between samples (damaged, healed)

In the case of the damaged sample, the corrosion potential and current was determined to be around -0.55 V (vs Vref) and $10^{-3.95}$ A/cm^2. After healing of the damaged sample, the corrosion potential and current was determined to be around -0.40 V (vs Vref) and $10^{-4.3}$ A/cm^2.

The corrosion potential of the healed coating on the stainless steel was -0.15 V (vs Vref) higher than the damaged coating on the stainless steel, and the corrosion current of the coated sample was less than the damaged one.

Therein, it can be concluded that the healed coating on the stainless steel could prevent a corrosion reaction between the electrolyte and the stainless steel, and become more resistant to corrosion than the damaged sample. This result shows that the damaged area by the sharp blade was re-established by forming the protective layer to corrosion.

4.2.3. **Comparison of potential dynamic test between all samples**

Figure 36 shows the comparison of the corrosion potential and the corrosion current between the samples (bare, coated, damaged and healed coating on stainless steel). It is obvious that bare stainless steel shows lower corrosion potential and higher corrosion current than coated one, which means coated sample is more resistant to corrosion. Nano-structured coating can prevent a corrosion reaction that is electron transfer between the stainless steel substrate and the corrosive environment.

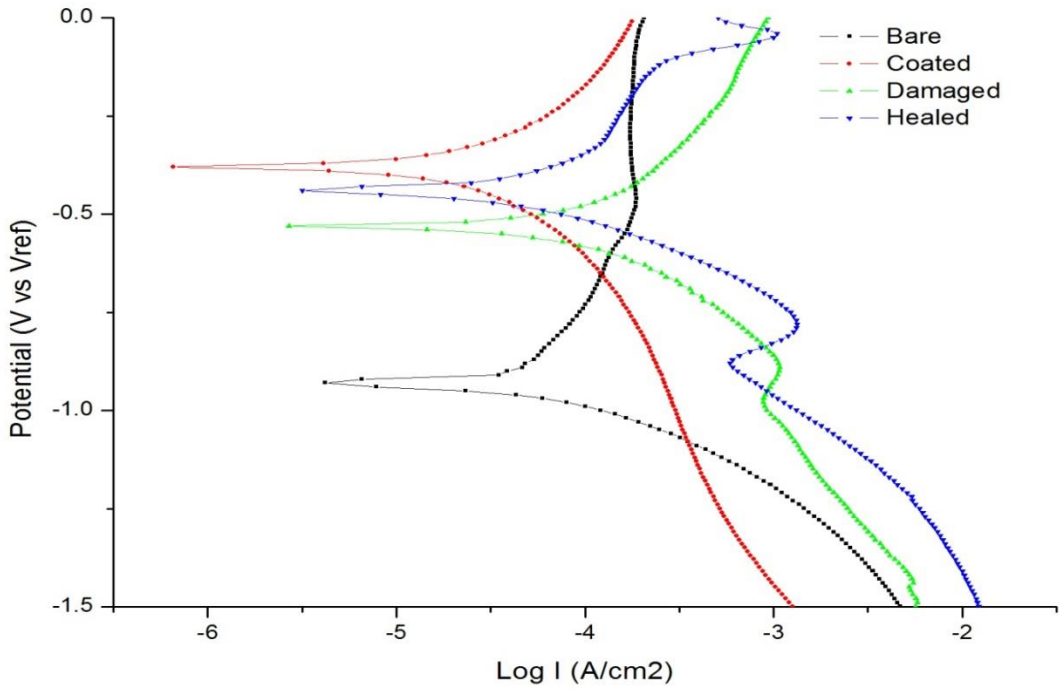

Figure 36. Comparison of the corrosion potential and current between samples (bare, coated, damaged, healed coating on the stainless steel)

A coating on substrate, damaged by scratching with a sharp blade, shows lower corrosion potential than coated stainless and higher corrosion potential than bare stainless steel, which means damaged coating can prevent corrosion but not much as the perfect coating. The damaged coating on the metal substrate makes the stainless steel exposed to the corrosive environment and caused corrosion of it. Therein, the corrosion potential of the damaged sample became lower than the coated sample.

After damaged coating is repaired under ultraviolet light for 15 minutes with 255 nm wavelengths, the corrosion potential becomes higher than the stainless steel with damaged coating, which means the new passivation layer is generated on the damaged

spot of the coating and prevents the corrosion reaction on surface of stainless steel substrate. The protective passivation layer can be considered as the chelated layer; that is the strong and dense coordination complex molecules layer which can deactivate the metal ion (M^{n+}) and avoids attacking for corrosion with other elements to produce the metal rust. The chelated layer can be described as the three coordinate bonds formation between a metal ion in the core and polydentate ligands of 8 HQ in the outer [52].

4.3. EIS analysis

Figure 37 shows the nyquist plot for each sample (bare, coated, damaged and healed) to evaluate the surface configuration (circuit model).

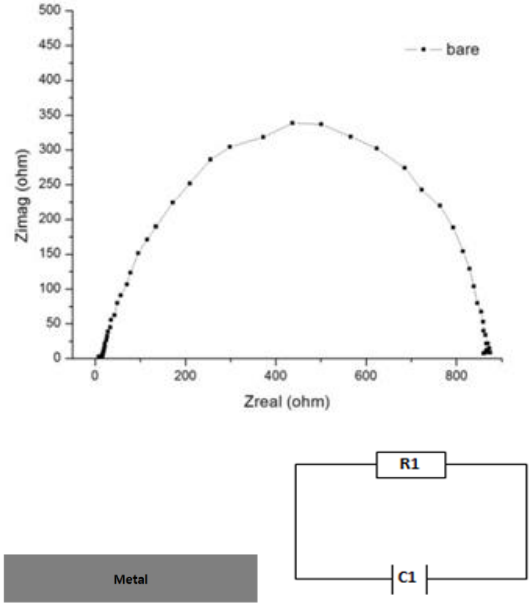

< Bare sample >

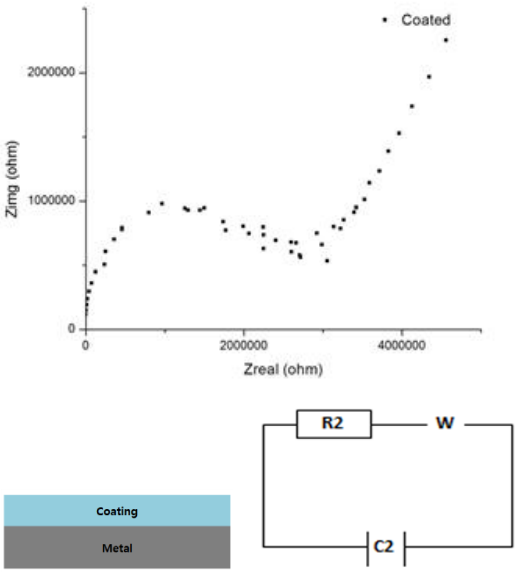

< Coated sample >

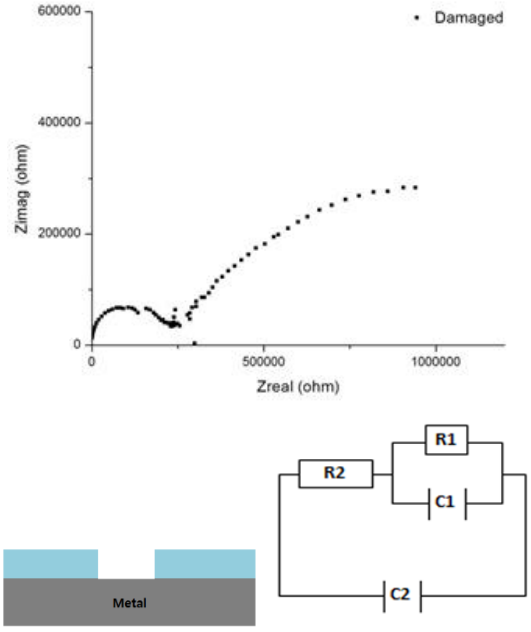

< Damaged sample >

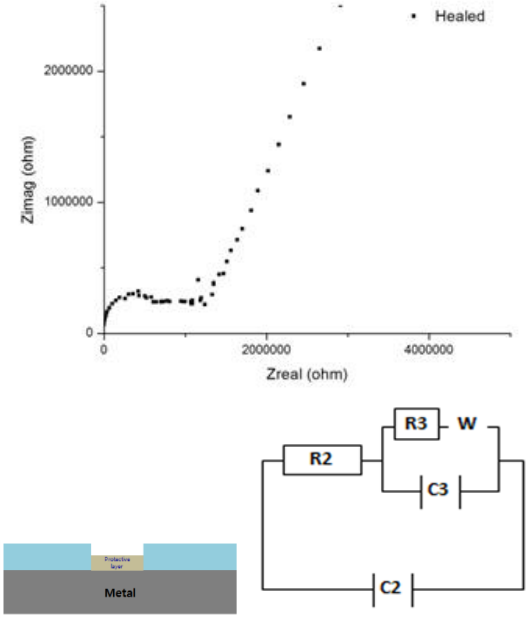

< Healed sample >

Figure 37. The Nyquist plot and the surface circuit model for each sample

In case of the bare metal, the nyquist plot indicates the sample behaves as semi-circle. This means that the resitance R (charge transfer) and C (Capacitance) component existed on the surface. It is possible to expect that the double layer by oxidation on the stainless steel surface was generated.

In case of the coated sample, the nyquist plot shows Warburg impedance at low frequency area, which means the diffusion (ionic transfer) from the electrolyte solution to the active nano-structured coating. It is possible that corrosion reaction (electrochemical) on the stainless steel surface was protected by the coating.

In case of the scratched sample, the nyquist plot shows two different kinds of the double layers on the stainless steel surface, which indicate the damages of the coating exposed to the electrolyte solution and further corrosion was observed.

In case of healed sample, the nyquist plot shows two different kinds of the double layers on the surface. However, these double layers show the Warburg impedance, which means the diffusion dominates from the electrolyte solution to the coating. This result indicates that the new protective layer for corrosion was generated by the chelating reaction with the metal ions and the corrosion inhibitors.

The generated interfacial double layers are expected to be around ZnO nanoparticles in the coating [53-55]. The active nano-structured coating makes it possible to form the double layers further, which cause the diffusion process. The straight line at right side of the nyquist plot (low frequency area) of the coated sample shows the Warburg impedance.

Figure 38 shows the comparison of the nyquist plot for evaluating corrosion resistivity for all samples tested in this research. As shown in this figure, the bare sample shows significantly low resistance value, and the coated sample shows highest resistance value between the electrolyte and the surface of the sample. Showing high resistance value means that the electrochemical reaction on the surface is difficult to happen. Corrosion can be explained as electrochemical reaction between a material and environment, thus it is obvious that the active nano-structured coating prevents the corrosion reaction of the stainless steel metal substrate.

The healed sample shows the higher value of resistance than damaged sample. It means that the damaged coating was reconstructed by forming the protective layer. The formed layer is protective for the electrochemical reaction, i.e., corrosion, between the surface of the sample and the electrolyte.

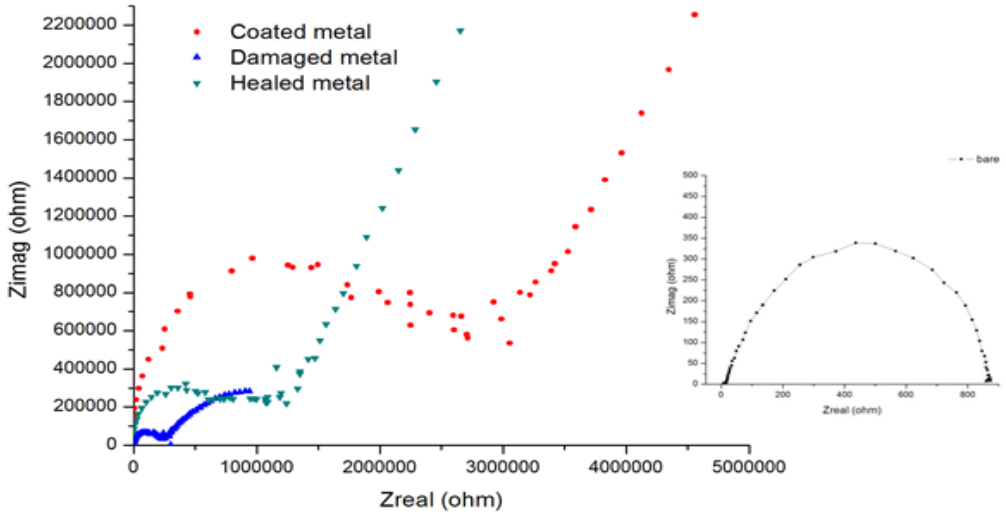

Figure 38. The comparison of the nyquist plots for evaluating corrosion

4.4. The mechanisms of the active nano-structured coating for corrosion protection

4.4.1. Photo-reaction

The strategy for anti-corrosion and self-healing coating is the active nano-structured layer-by-layer coating consisted of photo-catalytic material, corrosion inhibitor and poly-electrolytes. Photo-catalytic metal nano-particle is the key material for self-healing mechanism. When a photo-catalytic material absorbs ultraviolet (UV) light from light source, an electron density of the photo-catalytic material is changed from valence band to conduction band by photon energy. It also produces the pairs of electrons and holes simultaneously [56].

Figure 39 shows the schematic of photo-reaction on photo-catalytic reaction under ultraviolet light of Zinc oxide. This reaction on photo-catalytic material can establish the condition for self-healing coating. Also, excited electron (e-) and positive hole (h+) by photo-reaction react with surroundings and create photo-reduction and photo-oxidation processes [56].

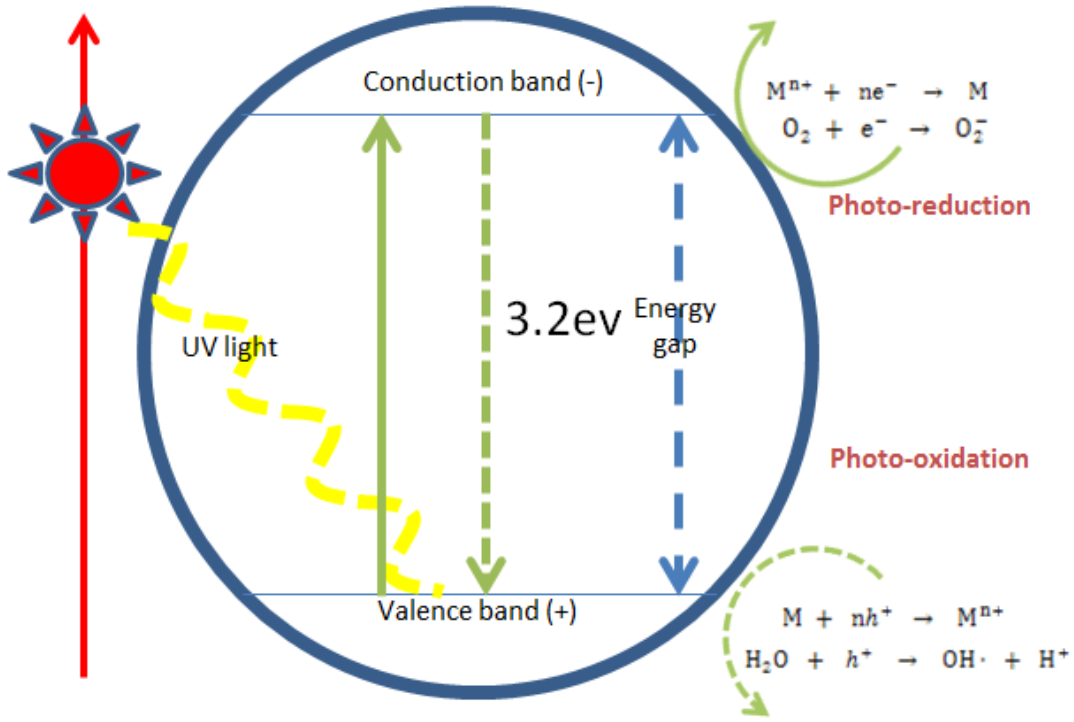

Figure 39. Schematic of photo-reaction on photo-catalytic material

An energy gap of materials (between valence band and conduction band) is called band gap that is the factor to distinguish between a conductor, a semiconductor and an insulator for identifying electric conductivity [1]. If a band gap does not exist, this material would be a conductor. If there is a large band gap, this material would be an insulator. If there is a small band gap, this material would be a semiconductor. Photo-catalytic material, which has small band gap, would be a kind of semiconductor because the electron density can be changed from one state (valence band) to another state (conduction band) by the external stimuli such as doping or ultraviolet light radiation [57].

Figure 40 shows the excited electron density under ultraviolet light on the photo-catalytic material (Zinc oxide) of the active nano-structured coating which will be introduced in this research.

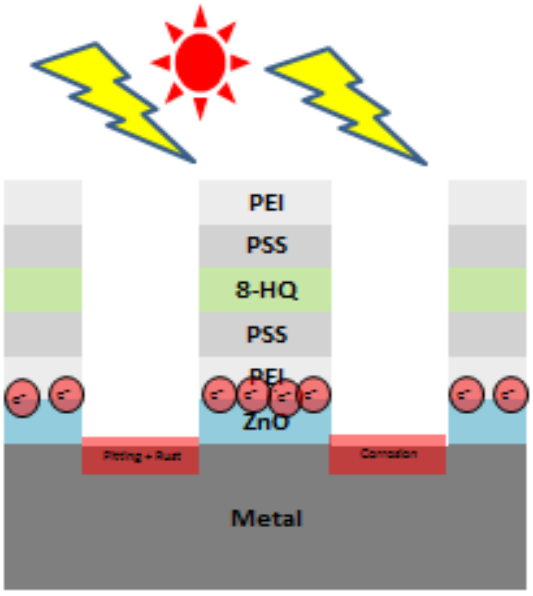

Figure 40. Excited electron density under ultraviolet light on the photo-catalytic material (Zinc oxide) of the active nano-structured coating

4.4.2. **Mechanisms of self-healing coating under UV light**

The excited electron density under ultraviolet light in photo-catalytic materials acted to form the protective layer. The exited electron density made changes of the electron density of the poly-electrolytes, and the corrosion inhibitor encapsulated in poly-electrolytes was released into the damaged area of the coating. Then, the formation of the chelation on surface made the passivation layer and protects corrosion reaction of

the substrate [58]. The chelated passivation layer is the highly bonded coordination complex and has been used for the dense and resistant layer of corrosion widely [59]. Figure 41 shows chelate reaction between complex metal ion and polydentate ligands to form a protective layer for corrosion.

$$M^{n+} + 8\ HQ\ (\text{corrosion inhibitor}) \rightarrow Mqn \quad (8)$$

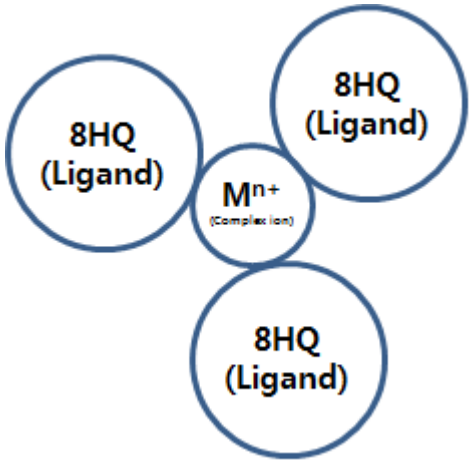

Figure 41. Chelate reaction between metal complex ion and ligands

4.4.3. **Configuration of anti-corrosion and self-healing coating**

The configuration of the active nano-structured coating for anti-corrosion and self-healing is described in Figure 42. The layer-by-layered active nano-structured coating prevented corrosion reaction of the substrate. Once the coating was damaged, corrosion happened on bare metal under corrosive environment. Then, damaged area was reconstructed by forming the chelated layer, which is protective for corrosion

reaction of the metal substrate [59]. This is self-healing mechanism of the active nano-structured coating for corrosion under ultraviolet light irradiation.

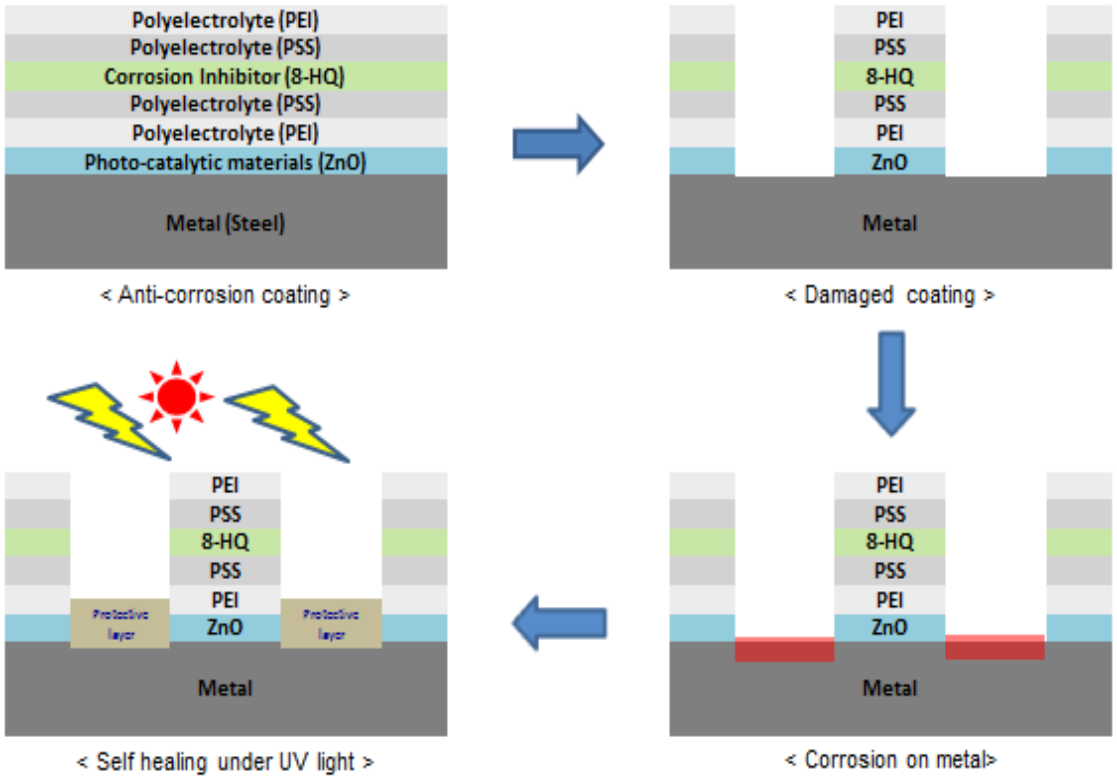

Figure 42. Configuration of active nano-structured coating for anti-corrosion and self-healing

4.5. Summary

In order to evaluate the corrosion resistivity and self-healing effect of the active nano-structured coating on the stainless steel substrate, the potential dynamic tests were performed. The corrosion potential values can determine when the anodic reaction on the surface of materials dominates the cathodic reaction. The anodic reaction means that

the surface of metal decomposes into metal ions and electrons, and this process causes pitting by corrosion.

The corrosion potential of the coated sample showed much higher value than the non-coated sample. This means that the active nano-structured coating prevented the corrosion reaction on the stainless steel surface. The zinc oxide nano-powder and the corrosion inhibitors fabricated on the stainless steel surface acted as the barrier for the chemical reaction between the surface of the sample and the electrolyte, which was used in this research.

Once the coating was scratched by the sharp blade, this sample was exposed to the corrosive environment and was expected to corrode. Afterwards, the damaged sample was healed under the ultraviolet light, which causes the photo-reaction of the zinc oxide nano-powders layer on the stainless steel substrate to make the protective layer for corrosion. This process was proven by the result of the potential dynamic tests of the damaged sample and the healed sample. The corrosion potential value of the healed sample was higher than the damaged sample.

CHAPTER V

ACTIVE COMPOSITE COATING FOR WEAR RESISTANCE

This chapter discusses the active nano-structured composite coating for wear resistance. To evaluate the active composite coating for wear resistance, hardness test, wear test and friction coefficient test were performed.

5.1. Evaluation of hardness

Figure 43 and Table 1 shows the comparison of the Rockwell hardness value (HRC) of the carbon steel substrate before and after the active composite coating. The coated sample with the composite materials showed higher hardness than the non-coated sample. The composite materials re-acted with the surface of the carbon steel substrate at relatively low temperature and made the new surface with higher hardness than non-coated carbon steel. The aluminum nano-powers and sodium nitrate behaved as a heat ignition and a releasing agent. The tungsten and graphite strengthened the carbon steel surface due to their own properties. The materials with high hardness were expected to have high wear resistance as well.

In order to calculate how much the hardness of the sample was increased by the active composite coating, the following equation was used.

$$H_{increased}(\%) = \frac{H_{after} - H_{before}}{H_{before}} \times 100 \quad (9)$$

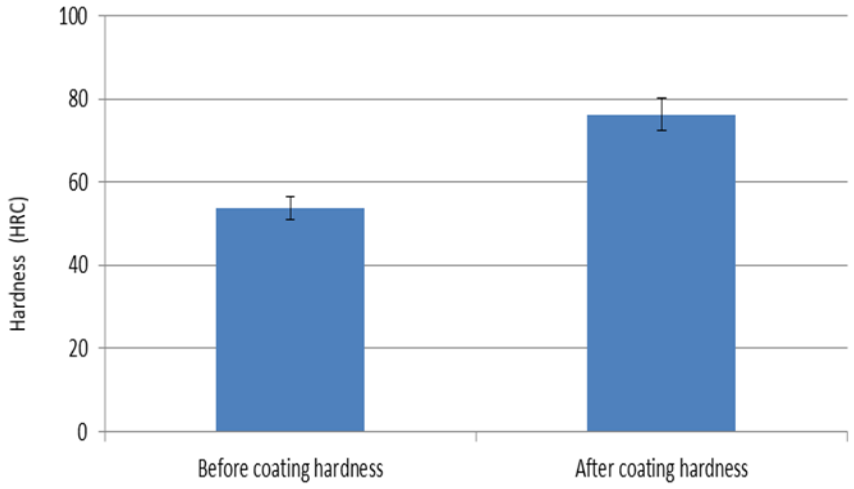

Figure 43. Comparison of the hardness before and after the active composite coating

Table 1. The hardness values of each measurement of the sample (before and after the active composite coating)

Hardness	1st	2nd	3rd	4th	5th	average
Before coating hardness	52.6	53.7	54.5	53.9	54.2	53.78
After coating hardness	77.1	73.7	75.6	78.1	76.6	76.22

By equation (9), $H_{increased}(\%) = \frac{76.22 - 53.78}{53.78} \times 100 = 41.7255\ (\%)$ was calculated. It is obvious that the active composite coating made the carbon steel substrate 41.7255 (%) harder than the non-coated sample.

Materials can become physically harder through the hardening processes, which mean they go through a metallurgical process to enhance the hardness that is related

with Young's modulus of the metal. For instance, as a metal has a high Young's modulus and yield stress, it is possible to say that the metal has a high hardness as well as a high resistance to plastic deformation. Hence, in order to increase wear resistance on a surface of a metal, the metal needs to become harder than before.

5.2. Evaluation of wear resistance

Figure 44 and Table 2 shows the comparison of the wear rate of the carbon steel substrate before and after the active composite coating. The coated sample with the composite materials showed lower wear rate than the non-coated sample. As discussed before, the materials having higher hardness are expected to have higher wear resistance because a wear, in other words a plastic deformation, on the surface of a metal is strongly related to and proportional with the surface hardness of a metal. From this point, we could assume that the wear resistance of the coated sample would be higher than the wear resistance of the non-coated sample, and this assumption was proven by this data in Figure 44 and Table 2.

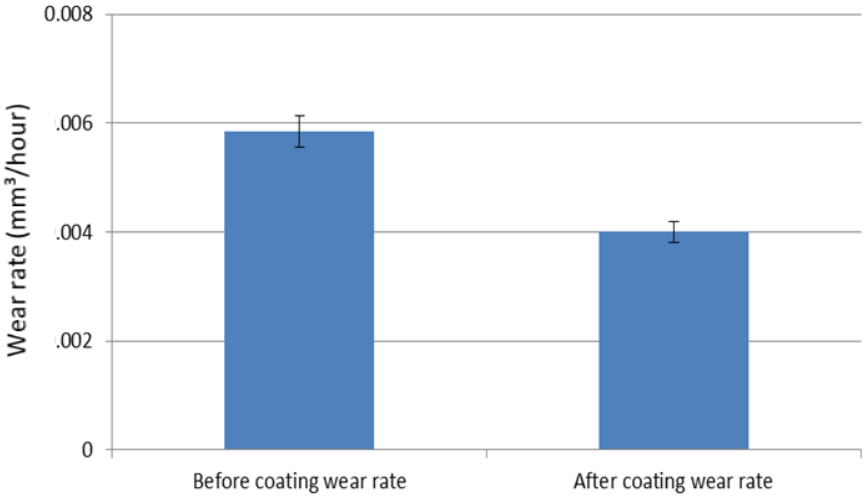

Figure 44. Comparison of the wear rate before and after the active composite coating

Table 2. Wear rate parameters of each measurement of the sample (before and after the active composite coating)

Before coating	1st	2nd	3rd	4th	5th	average
Wear depth (mm)	4.50E-03	4.00E-03	3.50E-03	4.00E-03	3.50E-03	0.0039
Wear width (mm)	0.32	0.3	0.3	0.32	0.26	0.3
Wear length (mm)	10	10	10	10	10	10
Duration (2 hours)	2	2	2	2	2	2
wear rate (mm^3/h)	0.0072	0.006	0.00525	0.0064	0.00455	0.00585

After coating	1st	2nd	3rd	4th	5th	average
Wear depth (mm)	2.50E-03	2.80E-03	3.00E-03	3.80E-03	2.50E-03	0.00292
Wear width (mm)	0.27	0.28	0.26	0.3	0.26	0.274
Wear length (mm)	10	10	10	10	10	10
Duration (2 hours)	2	2	2	2	2	2
wear rate (mm^3/h)	0.003375	0.00392	0.0039	0.0057	0.00325	0.004

In order to calculate how much the wear resistance of the sample was improved by the active composite coating, the following equation was used.

$$W_{decreased}(\%) = \frac{W_{before} - W_{after}}{W_{after}} \times 100 \quad (10)$$

And the wear rate of the sample was calculated by this equation. Wear rate of the carbon steel can be determined simply by multipling the wear depth, wear width and wear length of the wear scar generated by the hard material.

$$Wear\ rate_{sample}(\frac{mm^3}{h}) = \frac{Wear_{depth} \times Wear_{width} \times Wear_{length}}{Sliding\ hour} \quad (11)$$

Figure 45 shows the wear parameters such as wear length, width and depth to calculate the wear rate of the sample in this research. Volume is in three dimensional values: m^3, ft^3 or qt. When the hard material scratches over the carbon steel substrate, the wear scar is generated depending on a hardness of material, an applying force and duration of scratching. In this research, the 6mm diameter of the stainless bearing ball scratched over the carbon steel with 8 lb and 2 hours. As the shape of the stainless steel ball is a sphere, the shape of the wear scar is expected to be a semi-circled cylinder.

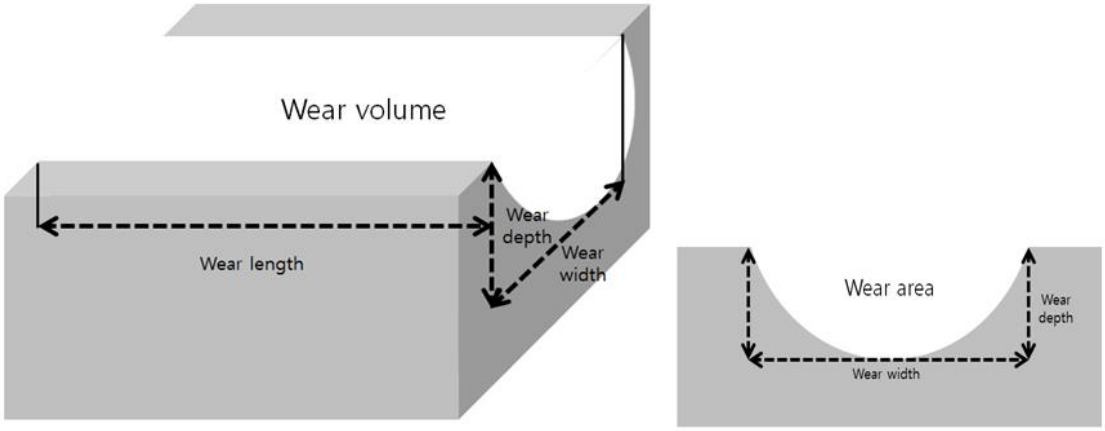

Figure 45. The wear geometry on the substrate by friction of the stainless ball bearing

In order to measure the wear rate of the carbon steel substrate, the surface interferometer was used. As mentioned in CHAPTER III, the surface interferometer is suitable equipment to examine the surface map such as morphology and roughness. The visulaized 2D and 3D images also make it easy for us to recongnize the surface map.

Figure 46 shows the optical microscope of wear track images before and after coating. As shown by this figure, the wear scar of the non-coated sample shows bigger wear scar than the coated sample. It means that the coated sample shows higer the wear resistace than the non-coated sample.

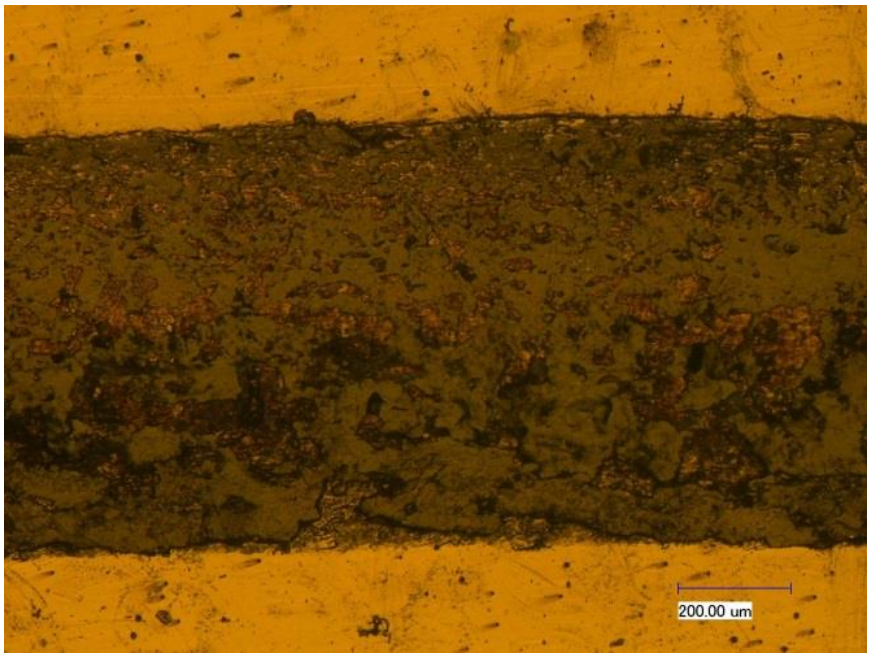

< Before the active composite coating >

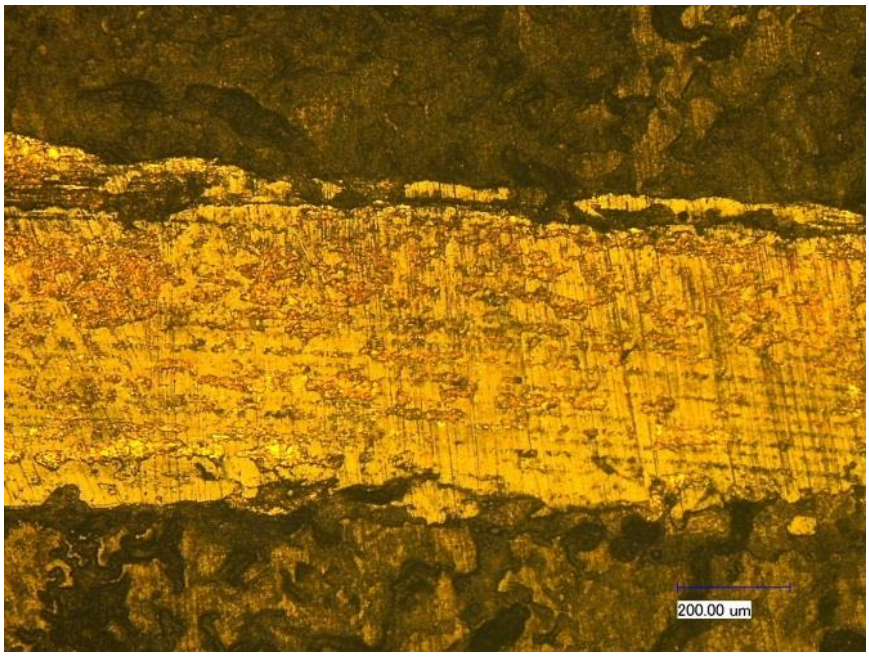

< After the active composite coating >

Figure 46. The surface interferometer test on the wear scar before and after coating

Figure 47 shows the result of the surface interferometer test on the wear scar to calculate the wear parameter such as the wear depth and the wear width before and after coating. Wear width was determined by the X axis of the surface profile data, which is the length of the dotted white line between the two peaks. Wear depth also was determined by the Y axis of the surface profile data, which is the length of the dotted yellow line under the white line. As shown by these data, the wear scars were generated by scrubbing, and the shape of wear area was semi-circled as we expected.

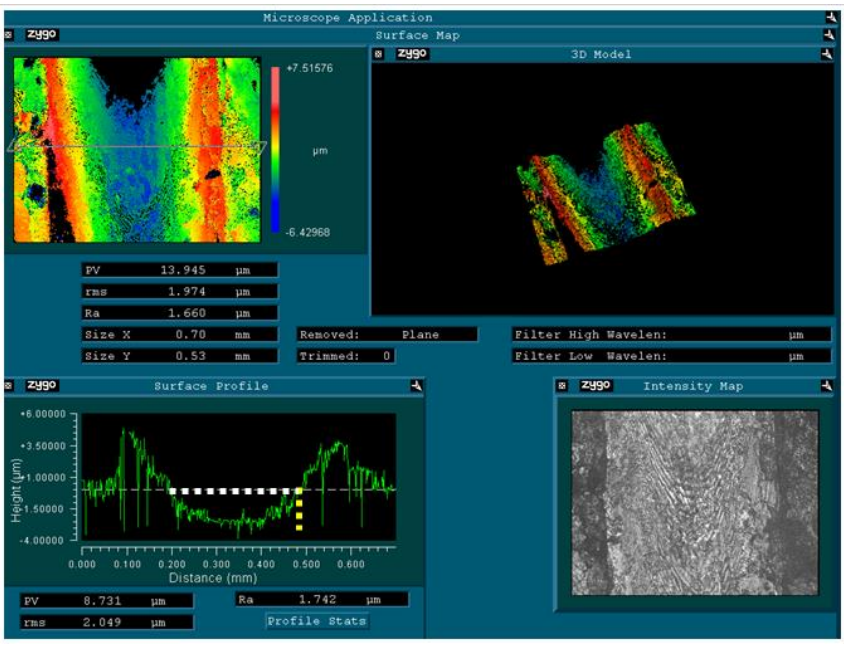

< Before the active composite coating >

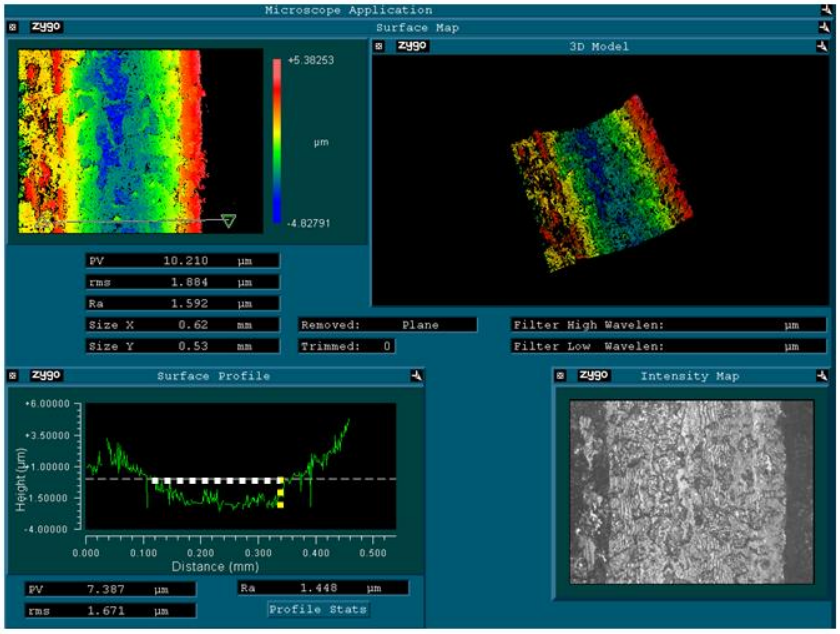

< After the active composite coating>

Figure 47. The surface interferometer test on the wear scar before and after coating

By equation (11), the wear rate of the samples, both before and after coating, was calculated. It revealed that the wear rate of the coated sample was 0.00400 (mm^3/h), and the wear rate of the non-coated sample was 0.00585 (mm^3/h).

By equation (10), $W_{decreased}(\%) = \frac{0.00585 - 0.00400}{0.00400} \times 100 = 46.25\ (\%)$ was calculated. It is obvious that the active composite coating made the carbon steel substrate 46.25 (%) more resistant for wear rate than the non-coated sample, and it was almost proportional to increased percentages of the hardness values of the samples between before and after coating.

It can be concluded that the active composite coating which were composed of the heat ignition / releasing agents and the surface modifiers make the surface of carbon steel harder by hardening processes, and the surface of carbon steel became more resistant for wear when comparing the samples before and after coating.

5.3. Evaluation of friction coefficient

As explained in CHAPTER III, in order to measure the friction coefficient of the samples, the tribometer was used. Applied force was 4N, and friction coefficient can be calculated by equation (8).

$$\text{Friction efficient } (\mu) = \frac{Friction\ force\ (N)}{Applied\ forece\ (N)} \quad (12)$$

Figure 48 illustrates the schematic of measuring friction coefficient data between the two different solid surfaces, which is dry friction measurement, in this research. When an opposite material touches and scrubs on a substrate with applied force, friction force is generated corresponding to several parameters, such as scratching speed,

distance and environment factors. The friction energy between the two solid surfaces can be changed into thermo energy, which is heat. The friction energy also causes the plastic deformation, which is wear, on the surface of the softer material.

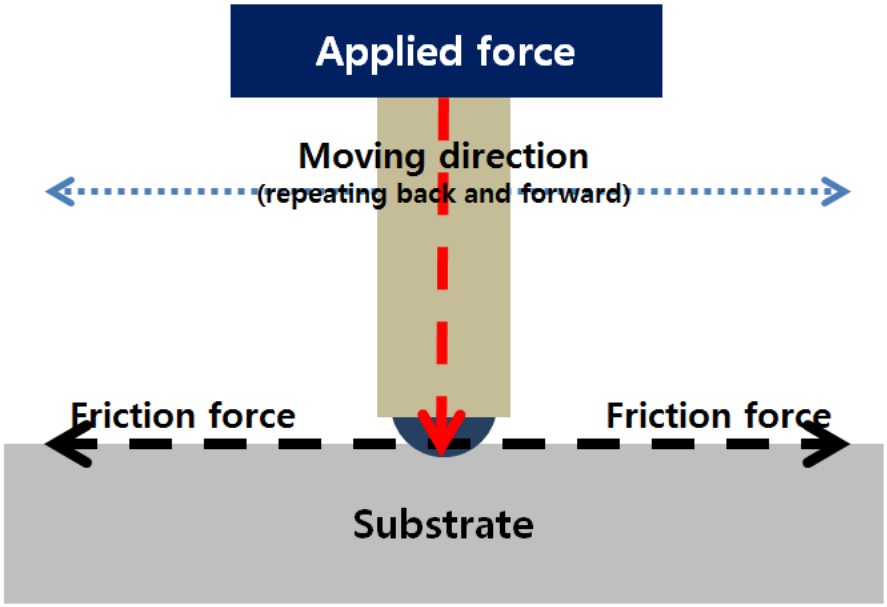

Figure 48. Schematic of measuring friction coefficient of the sample

Figure 49 shows the result of friction coefficient data before and after the active composite coating. The friction coefficient of non-coated sample was 0.412 while the friction coefficient of coated sample was 0.363. The difference of friction coefficient between the two samples, coated and non-coated, was only 0.049. Therein, it can be concluded that there was not much difference of friction coefficient data between the two samples. This result indicates that the friction coefficient is not a function of surface hardness or a composition of materials. The surface roughness can affect friction

coefficient data since the friction forces of the two samples are similar. Friction force can be described as resistance force against sliding of the stainless steel ball.

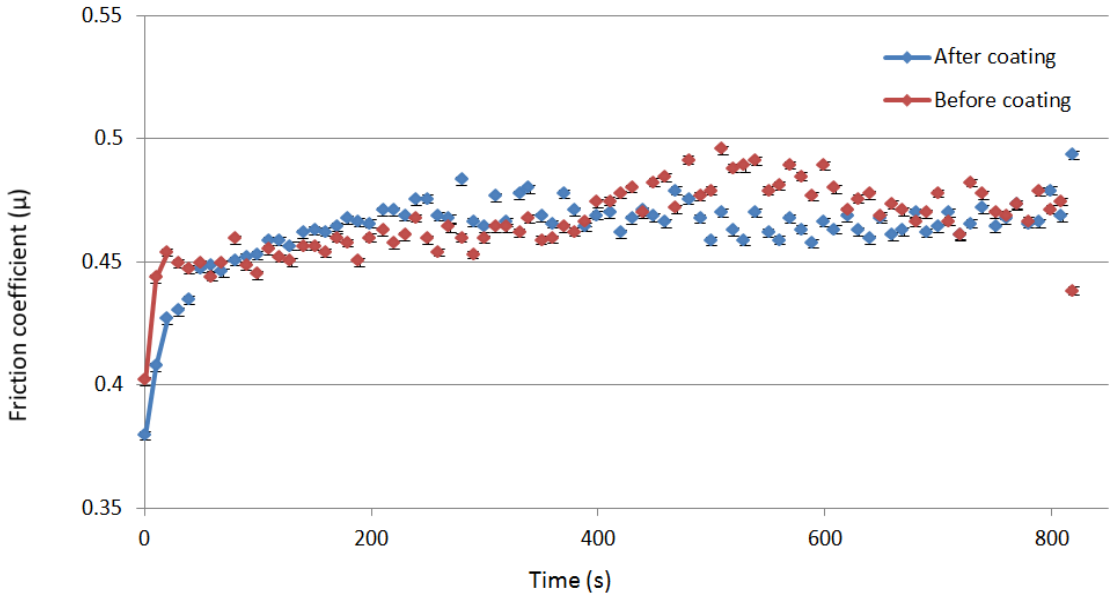

Figure 49. Comparison of the friction coefficient before and after the active composite coating

5.4. The mechanism of the active composite coating for wear protection

In order to improve wear resistance of high carbon steel, composite materials were used for the surface coating. The composite materials consisted of heat ignition / releasing agents and surface modifier. The heat ignition / releasing agents were the nano-sized materials and were reacted at relatively low temperature due to their higher chemical reactivity [31]. The surface modifiers which have high strength and hardness were used to make the steel surface harder and more resistant for wear.

The carbon steel substrate was covered with the composite materials uniformly and the heat treatment was performed under a certain temperature. During heat treatment, the composite materials react with the surface of substrate and the new surface, which has higher hardness and better anti-wear, was generated. Figure 50 shows the schematic of active nano composite coating on the surface of carbon steel.

Figure 50. Schematic of active nano composite coating

The hardening processes in this case of active composite coating would be described in two ways of hardening concepts. These concepts were a diffusion hardening and precipitation hardening under heat treatment. Basically, the hardening processes of metals can be performed by heat treatment. Heat on metals makes the hardening elements increase the chemical re-activity or diffuse into the substrate faster, or makes the micro-structure of metals change into another phase that has higher hardness and strength.

Firstly, diffusion hardening is the process when diffusion occurs between the composite materials and the carbon steel substrate. The carbon steel surface is modified by diffusion of the composite materials, which are composed of tungsten and graphite

powders. Increased heat in the furnace by heat ignition and releasing agents in the composite materials, which are aluminum nano-powders and sodium nitrate, makes the hardening elements in the composite materials diffuse into the surface of the substrate. For instance, the graphite powders structured with carbon atoms can be diffused into the surface of the substrate and the contents of the carbon elements are increased [60].

Secondly, precipitation hardening happens during the heat treatment by the composite coating materials. The modifiers, which are tungsten, graphite and iron, penetrate and are diffused into the surface of the carbon steel substrate. These entered particles of the modifiers on the surface of the substrate prevent the movement of dislocations of the metal substrate such as slip, or defects in a crystal's lattice. These particles act as impurities to impede the plastic deformation on the surface of metal, and this phenomenon makes the surface of metal harder. High temperature makes the modifier elements soluble into the surface of metal [61].

5.5. Summary

For evaluating the wear protection of the active composite coating on the carbon steel substrate, the Rockwell hardness tests and the wear rate calculations were accomplished. The results of hardness tests showed that the surface of the coated sample became harder than the non-coated sample by the hardening processes, such as precipitation and diffusion hardening. Furthermore, the wear rate of the coated sample was lower than the non-coated sample. This means that the active composite coating has wear resistance and protection ability on the surface of the carbon steel.

CHAPTER VI

CONCLUSIONS AND FUTURE RECOMMENDATIONS

6.1. Conclusions

This research explores nanostructured active coatings to protect corrosion and wear. Using experimental approaches, we introduced nano-materials to form coatings coating to protect corrosion and heal corroded surfaces. Due to the built-in mechanical properties, the wear resistance of the metal surface is improved.

The self-healable coating for corrosion protection proposed in this research was the active nano-structured coating, which was composed of photo-catalytic materials (ZnO), corrosion inhibitors (8 HQ) and polyelectrolytes (PSS and PEI). The coating on the metal substrate showed the anti-corrosion ability, and this coating was self-healable under ultraviolet light. When ultraviolet light irradiated to the coating on the metal, which were damaged by the sharp blade, the electron density of the Zinc oxide on the metal substrate was excited. By the excited electron density of the Zinc oxide, the electron density of the functional group of the polyelectrolytes was changed. This made it possible for the corrosion inhibitor to be released from the polyelectrolytes, which capsulated the corrosion inhibitor.

The corrosion resistivity of each sample was measured by the potential dynamic tests, and the results of the potential dynamic tests for each sample proved these mechanisms, anti-corrosion and self-healable effect of the active nano-structured

coating. Potential dynamic tests can measure the corrosion potential, which is the point to be happened the anodic reaction and cause corrosion pitting on the surface of metal.

The active composite coating for wear protection of the carbon steel was proposed in this research. For the construction of anti-wear coating on the the carbon steel surface, the mixed composite materials, which consisted of the aluminum nano-powder, sodium nitrate, tungsten power, graphite powder and iron powder, were presented.

The composite materials re-acted with the surface of the carbon steel by the heat treatment, and the newly coated surface was produced. By hardness and wear testing on the carbon steel sample, it was revealed that the coated sample had higher hardness values and lower wear rate than non-coated sample.

This research is expected to help reducing cost and safety hazard related with corrosion and wear on metal surfaces. Using nanostructured materials to engineer and protect surfaces of metals is a novel approach. It opens areas for future investigation, and here proposed the active nano-structured composite coating showed the feasibility enough to be industrialized or technologically advanced further.

6.2. Future Recommendations

1. The tribological tests of the active nano-structured coating, for example friction test and wear test, need to be conducted to evaluate the mechanical properties of the coating.

2. The other test such as the wettability test and corrosion test need to be performed to identify the surface properties of the active composite coating.

3. The potential application need to be carried out by modeling and designing.

REFERENCES

[1] William D. Callister J. Materials science and engineering an introduction. 7th ed: John Wiley and Sons, Inc. New York, NY. 2007.

[2] Speidel M, Hyatt M. Stress-corrosion cracking of high-strength aluminum alloys. In: Fontana M, Staehle R, editors. Advances in corrosion science and technology: Springer New York, NY; 1972. p. 115-335.

[3] DuQuesnay DL, Underhill PR, Britt HJ. Fatigue crack growth from corrosion damage in 7075-T6511 aluminium alloy under aircraft loading. International Journal of Fatigue. 2003;25:371-7.

[4] Bennett LH, Kruger J, Parker RL, Passaglia E, Reimann C, Ruff AW, et al. Economic effects of metallic corrosion in the United States. Report to the Congress; Related Information: NBS Special Publication 511-1. Part 1. 1978.

[5] Hendricks W. The aloha airlines accident-A new era for aging aircraft. In: Atluri SN, Sampath SG, Tong P, editors. Structural integrity of aging airplanes: Springer Berlin Heidelberg; 1991. p. 153-65.

[6] Pyles, Raymond A. Aging aircraft: USAF workload and material consumption life cycle patterns. Santa Monica, CA: RAND Corporation, 2003.

[7] Magazine ANaRO. Lessons from aloha by Martin Aubury, Available from http://avstop.com/stories/aloha.html (access date: June 27, 2013).

[8] David Kennedy YX, Emilia Mihaylova. Current and future applications of surface engineering. The Engineers Journal (Technical). June, 2005;Vol.59, p. 287-292.

[9] Davis JR. Surface engineering for corrosion and wear resistance, Introduction to surface engineering for corrosion and wear resistance. Materials Park, OH: ASM International; 2001, p. 1-10.

[10] Davis JR. Corrosion: Understanding the basics (#06691G),The effects and economic impact of corrosion. Materials Park, OH: ASM International; 2000, P. 1-20.

[11] Koch GH. Corrosion costs and preventive strategies in the United States; Washington DC, Department of Transportation. 2001.

[12] Kolesar SC. Principles of corrosion. Reliability Physics Symposium, 1974 12th Annual1974. p. 155-67.

[13] Wessling B, Posdorfer J. Corrosion prevention with an organic metal (polyaniline): corrosion test results. Electrochimica Acta. 1999;44:2139-47.

[14] Grundmeier G, Schmidt W, Stratmann M. Corrosion protection by organic coatings: electrochemical mechanism and novel methods of investigation. Electrochimica Acta. 2000;45:2515-33.

[15] Hubrecht J, Vereecken J, Piens M. Corrosion monitoring of iron, Protected by an organic coating, with the aid of impedance measurements. Journal of The Electrochemical Society. 1984;131:2010-5.

[16] Steijn RP. The sliding surface of polytetrafluoroethylene: an investigation with the electron microscope. Wear. 1968;12:193-212.

[17] Andreeva DV, Skorb EV, Shchukin DG. Layer-by-layer polyelectrolyte/inhibitor nanostructures for metal corrosion protection. ACS Applied Materials & Interfaces. 2010;2:1954-62.

[18] Rabinowicz E. Friction and wear of materials. 2nd edition: John Wiley and Sons, Inc. New York, NY. 1995.

[19] B. S. Hockenhull EMKaPLBO. Predicting wear for metal surfaces in sliding contact using a low-cycle fatigue wear model. J Appl Mech. 1993.

[20] Williams JA. Wear and wear particles - Some fundamentals. Tribology International. 2005;38:863-870.

[21] Bayer RG, Schumacher RA. On the significance of surface fatigue in sliding wear. Wear. 1968;12:173-83.

[22] Waterhouse RB. Fretting wear. Wear. 1984;100:107-18.

[23] Jones M, H., and D. Scott, Eds. Industrial Tribology: the practical aspects of friction, lubrication, and wear. New York: Elsevier Scientific Publishing Company; 1983.

[24] Wang CH. Introduction to fracture mechanics. Melbourne, Vic.; DSTO Aeronautical and Maritime Research Laboratory. 1996.

[25] M.S. Rosenfeld. Damage tolerance in aircraft structures-Stp 486. Lutherville-Timonium, Md.: ASTM International; 1971.

[26] Koellhoffer L, Manz AF, Hornberger G. Welding processes and practices: John Wiley and Sons, Inc. New York, NY. 1987.

[27] Eranna G. Advantages of Nanomaterials. Metal Oxide Nanostructures as Gas Sensing Devices: Taylor & Francis, Boca Raton, FL; 2011. p. 27-38.

[28] Youssef KM, Scattergood RO, Murty KL, Horton JA, Koch CC. Ultrahigh strength and high ductility of bulk nanocrystalline copper. Applied Physics Letters. 2005;87:091904--3.

[29] Naser Belmilouda A-HT, Paul W. Mertensa, Xiumei Xua and Herbert Struyf. Investigation on the drying dynamics of millimetric water droplets: Source of Watermarks on Silicon Wafers. The Electrochemical Society. 2011.

[30] Rai A, Park K, Zhou L, Zachariah MR. Understanding the mechanism of aluminium nanoparticle oxidation. Combustion Theory and Modelling. 2006;10:843-59.

[31] C. N. R. Rao AM, Anthony K. Cheetham. The chemistry of nanomaterials: John Wiley and Sons, Inc. New York, NY. 2006.

[32] Morrow SJ. Materials selection for seawater pumps. Proceedings of the twenty-sixth international pump symposium. 2010.

[33] S.O. Fatin. HNL, W.T. Tan,N.M.,Huang. Comparison of photocatalytic activity and cyclic voltammetry of Zinc oxide and Titanium dioxide nanoparticles toward Degradation of Methylene Blue Int J Electrochem Sci, 7. 2012.

[34] Yu J, Yu X. Hydrothermal synthesis and photocatalytic activity of Zinc oxide hollow spheres. Environmental Science & Technology. 2008;42:4902-7.

[35] Tong H, Ouyang S, Bi Y, Umezawa N, Oshikiri M, Ye J. Nano-photocatalytic materials: Possibilities and Challenges. Advanced Materials. 2012;24:229-51.

[36] Ye J, Zou Z, Oshikiri M, Matsushita A, Shimoda M, Imai M, et al. A novel hydrogen-evolving photocatalyst InVO4 active under visible light irradiation. Chemical Physics Letters. 2002;356:221-6.

[37] Senadeera GKR, Kitamura T, Wada Y, Yanagida S. Deposition of polyaniline via molecular self-assembly on TiO_2 and its uses as a sensitiser in solid-state solar cells. J Photochem Photobiol, A. 2004;164:61-6.

[38] Andreeva DV, Shchukin DG. Smart self-repairing protective coatings. Materials Today. 2008;11:24-30.

[39] Wu DY, Meure S, Solomon D. Self-healing polymeric materials: A review of recent developments. Progress in Polymer Science. 2008;33:479-522.

[40] Jüttner K. Electrochemical impedance spectroscopy (EIS) of corrosion processes on inhomogeneous surfaces. Electrochimica Acta. 1990;35:1501-8.

[41] Mansfeld F. Electrochemical impedance spectroscopy (EIS) as a new tool for investigating methods of corrosion protection. Electrochimica Acta. 1990;35:1533-44.

[42] Cui G, Liu H, Wu G, Zhao J, Song S, Shen PK. Electrochemical impedance spectroscopy and first-principle investigations on the oxidation mechanism of hypophosphite anion in the electroless deposition system of Nickel. The Journal of Physical Chemistry C. 2008;112:4601-7.

[43] Gamry Instruments. Basics of electrochemical impedance spectroscopy. Application Note Rev. 1.0 9/3/2010.

[44] Mench MM, Kuo KK, Yeh CL, Lu YC. Comparison of thermal behavior of regular and ultra-fine Aluminum powders (Alex) made from plasma explosion process. Combustion Science and Technology. 1998;135:269-92.

[45] Freeman ES, Gordon S. The application of the absolute rate theory to the ignition of propagatively reacting systems. The thermal ignition of the systems Lithium Nitrate–Magnesium, Sodium Nitrate–Magnesium. The Journal of Physical Chemistry. 1956;60:867-71.

[46] Knowles PR. Design of structural steelwork. 2 nd ed: Taylor & Francis, Boca Raton, FL. 1987.

[47] Lassner ES, Wolf-Dieter. "low temperature brittleness". Tungsten: properties, chemistry. technology of the element, alloys, and chemical compounds Springer. 1999:20-1.

[48] Fee ELTA. Macroindentation hardness testing, ASM Handbook, Mechanical Testing and Evaluation. Materials Park, OH: ASM International; 2000.

[49] TechNotes C. Basics of Rockwell hardness testing, Available from http://www.ccsi-inc.com/t-rockwell1.htm (access date: June 27, 2013).

[50] Hilbert LR, Bagge-Ravn D, Kold J, Gram L. Influence of surface roughness of stainless steel on microbial adhesion and corrosion resistance. International Biodeterioration & Biodegradation. 2003;52:175-85.

[51] Jones DA. Principles and prevention of corrosion; 2nd edition. Prentice Hall, NJ. 1996.

[52] Cölle M, Dinnebierb RE, Brütting W. The structure of the blue luminescent delta-phase of tris(8-hydroxyquinoline) aluminium(III) (Alq_3). Chem Commun. 2002;2002:2908-9.

[53] Lozano-Castello D, Cazorla-AmorOsa D, Linares-Solanoa A, Shiraishib S, Kurihara H, Oya A. Influence of pore structure and surface chemistry on electric double layer capacitance in non-aqueous electrolyte. Carbon. 2003;41:1765-75.

[54] Lyklema J. The structure of the electrical double layer on porous surfaces. J Electroanal Chem. 1968;18:341-8.

[55] Yates DE, Levine S, Healy TW. Site-binding model of the electrical double layer at the oxide/water interface. J Chem Soc, Faraday Trans 1. 1974;70:1807-18.

[56] Scholes GD, Fleming, Graham R.,Olaya-Castro, Alexandra,van Grondelle, Rienk. Lessons from nature about solar light harvesting. Nat Chem. 2011;3.

[57] Hoffmann MR, Martin ST, Choi W, Bahnemann DW. Environmental applications of semiconductor photocatalysis. Chemical Reviews. 1995;95:69-96.

[58] Nagai R, Murray DB, Metz TO, Baynes JW. Chelation: A fundamental mechanism of action of AGE Inhibitors, AGE Breakers, and other inhibitors of diabetes complications. Diabetes. 2012;61:549-59.

[59] Norman Greenwood AE. Chemistry of the elements. 2nd ed. Oxford: Butterworth Heinemann; 1997.

[60] Todd RH, Allen DK, Alting L. Fundamental principles of manufacturing processes. 1st ed: Industrial Press Inc. New York, NY; 1994.

[61] William D. Callister J. Fundamentals of materials science and engineering. 2nd ed: John Wiley and Sons New York, NY. 2001.